



HAL
open science

Enantioselective iron-catalysed transformations. An update

Hélène Pellissier

► **To cite this version:**

Hélène Pellissier. Enantioselective iron-catalysed transformations. An update. Tetrahedron, 2024, 157, pp.133944. 10.1016/j.tet.2024.133944 . hal-04524283

HAL Id: hal-04524283

<https://hal.science/hal-04524283v1>

Submitted on 28 Mar 2024

HAL is a multi-disciplinary open access archive for the deposit and dissemination of scientific research documents, whether they are published or not. The documents may come from teaching and research institutions in France or abroad, or from public or private research centers.

L'archive ouverte pluridisciplinaire **HAL**, est destinée au dépôt et à la diffusion de documents scientifiques de niveau recherche, publiés ou non, émanant des établissements d'enseignement et de recherche français ou étrangers, des laboratoires publics ou privés.

Enantioselective iron-catalysed transformations. An update

Hélène Pellissier*

Aix-Marseille Univ., CNRS, Centrale Marseille, iSm2, Marseille, France

Contents

1. Introduction
2. Domino reactions
3. Reductions of ketones and imines
4. Cycloadditions
5. Additions to alkenes
6. Coupling reactions
7. Michael-type reactions
8. α -Functionalisations of carbonyl compounds
9. Sulfoxidations
10. Alkylations of indoles
11. Rearrangement reactions
12. Intramolecular aminations
13. Miscellaneous reactions
14. Conclusions

References and notes

*Corresponding author. Tel.: +33-4-13-94-56-41;

e-mail: h.pellissier@univ-amu.fr

Graphical Abstract

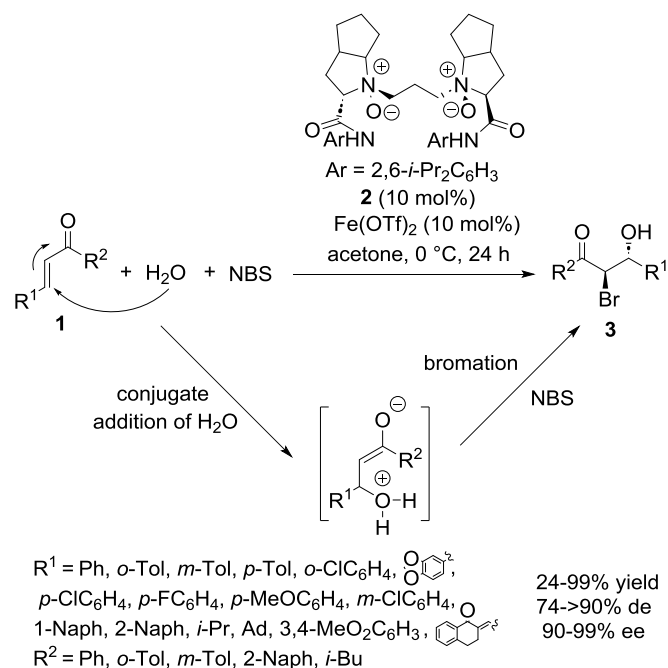
This review updates the field of enantioselective iron-catalysed transformations of all types since the beginning of 2020. It shows that asymmetric iron catalysis, that suits the growing demand for greener processes, offers a real opportunity to replace toxic and expensive metals

chiral iron complexes has allowed a wide diversity of greener asymmetric transformations to be achieved, leading to many types of chiral cyclic as well as acyclic products. Among highly enantioselective iron-catalysed reactions, are reductions of ketones and imines, additions to alkenes, coupling reactions, cycloadditions, Michael additions, cyclisations, epoxidations, ring-opening reactions, rearrangements, sulfoxidations, as well as more complex domino reactions. The goal of this review is to collect the recent advances in enantioselective iron-catalysed reactions of all types published since the beginning of 2020, as this field was most recently reviewed that year by Cera et al., including only 3 references published in 2020.³ Previously, this area was reviewed by different authors.⁴ In 2022, the use of octahedral and tetrahedral chiral iron complexes in asymmetric organic reactions was reviewed by Piarulli and Gazzola but including only 3 references ≥ 2020 .⁵ It must be noted that reactions promoted by multicatalytic systems including iron are not included in this review. The present review is divided into twelve parts, focussing successively on enantioselective iron-catalysed domino reactions, reductions of ketones and imines, cycloadditions, additions to alkenes, couplings, Michael-type reactions, α -functionalisations of carbonyl compounds, sulfoxidations, alkylations of indoles; rearrangement reactions; intramolecular aminations; and miscellaneous reactions.

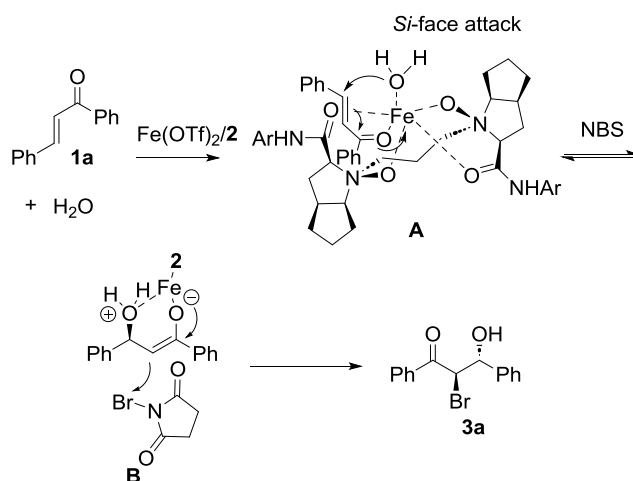
2. Domino reactions

One-pot methodologies allow a direct and economic access to complex chiral molecules by avoiding costly isolation and purification of intermediates.⁶ Among them are sophisticated domino reactions evolving under strictly the same reaction conditions.⁷ It must be recognised that so far, examples of asymmetric domino reactions catalysed by chiral iron complexes still remain rare. In an example reported in 2020 by Feng and Lin, substituted α,β -unsaturated ketones **1**, *N*-bromosuccinimide (NBS), and water were employed as substrates along with 10 mol% of a chiral iron catalyst (Scheme 1).⁸ The latter arose from the reaction between $\text{Fe}(\text{OTf})_2$ and chiral *N,N'*-dioxide ligand **2** in acetone at 0 °C within 24 hours. The enantioselective three-component bromohydroxylation process evolved through a domino Michael/ α -bromination reaction which resulted in the formation of chiral α -bromo- β -hydroxy ketones **3** with 90-99% ee, 74->90% de, and 24-99% yields. Lower yields (24-70% vs 81-99%) as well as lower de values (74->90% de vs >90-92% de) were observed in the reaction

of aromatic α,β -unsaturated ketones bearing sterically hindered *ortho*-substituted phenyl groups (R^1 or R^2) in comparison with substrates exhibiting *meta*- or *para*-substituted phenyl groups. Along with aryl-substituted enones ($R^1 = \text{aryl}$), good results (90-99% ee, 88->90% de, 45-52% yields) were also obtained in the reaction of alkyl-substituted substrates ($R^1 = \text{alkyl}$). A possible mechanism is proposed in Scheme 1, beginning with the formation of transition state **A** from the coordination of the ligand to the iron centre followed by that of enone and water. Then, this latter nucleophilic agent underwent conjugate addition through the less hindered *Si*-face of the enone reversibly which resulted in the formation of enolate intermediate **B**. The latter species subsequently reacted with Br^+ generated from the electrophilic trapping agent NBS from the opposite face to deliver the final product.

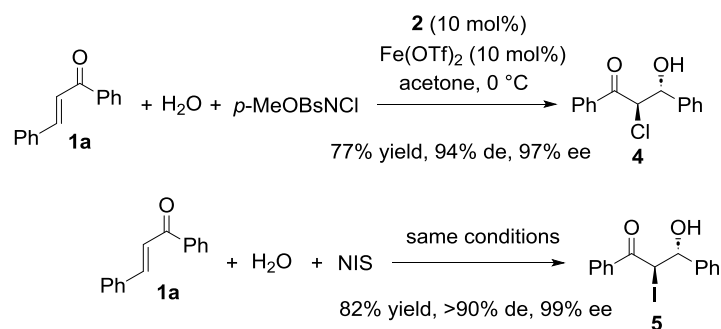


proposed mechanism (with $\text{R}^1 = \text{R}^2 = \text{Ph}$):



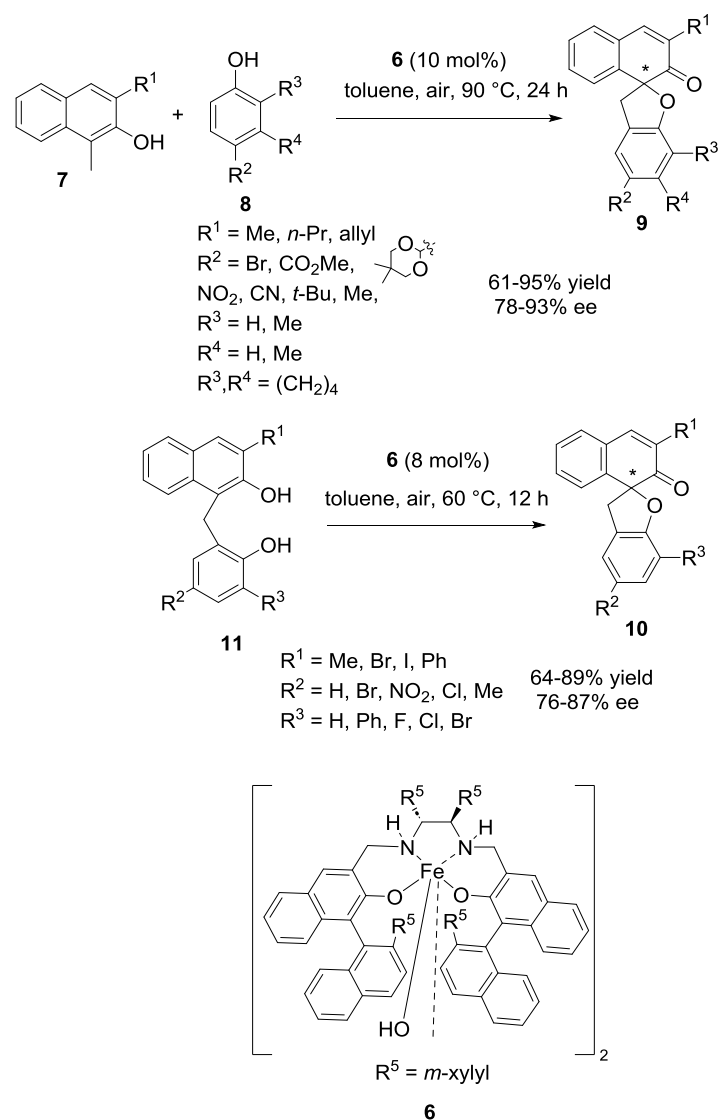
Scheme 1. Three-component bromohydroxylation reaction of α,β -unsaturated ketones with NBS and water.

The authors showed the compatibility of the precedent catalyst system to other electrophilic agents, such as $p\text{-MeOBsNCl}_2$ (Bs = benzenesulfonyl) as chloride source and N -iodosuccinimide (NIS) as iodide source (Scheme 2).⁸ The chlorohydroxylation reaction of $p\text{-MeOBsNCl}_2$ with chalcone **1a** and water led to chiral chlorohydroxylated product **4** with 97% ee, 94% de, and 77% yield. Similarly, the iodohydroxylation reaction between the same chalcone, water and NIS afforded chiral iodohydrin **5** in 99% ee, >90% de, and 82% yield.



Scheme 2. Three-component halohydroxylation reactions of chalcone and water with other halogenating agents.

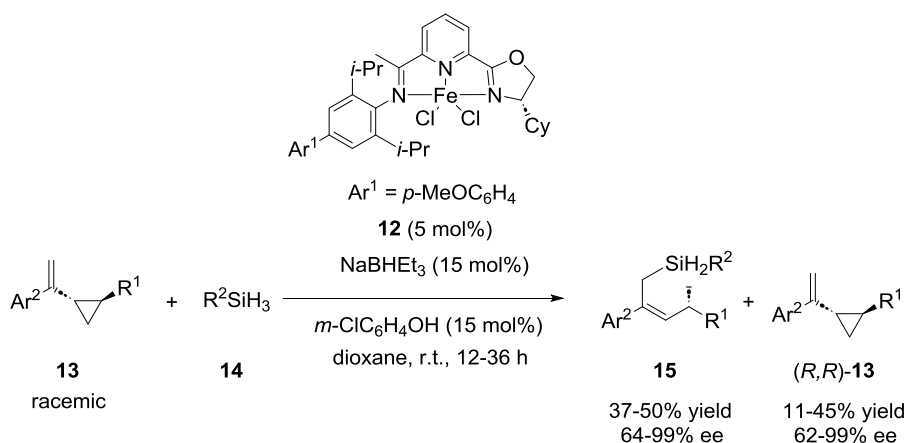
In 2020, an asymmetric domino reaction was developed by Uchida et al. in the presence of 10 mol% of chiral preformed iron catalyst **6**.⁹ It involved 1-methyl-2-naphthols **7** and phenols **8** as substrates which were heated at 90 °C in toluene under air. The enantioselective reaction evolved within 24 hours through oxidative dearomative spirocyclisation, affording chiral spirocyclic ketones **9** with 61-95% yields and 78-93% ee (Scheme 3). Furthermore, an intramolecular version of this reaction was developed at 60 °C by using only 8 mol% of the same catalyst. Both good enantioselectivities (76-87% ee) and yields (64-89%) were described for chiral spirocyclic ketones **10** arisen within 12 hours from the regioselective intramolecular domino reaction of methylenebis(arenol)s **11**.



Scheme 3. Intermolecular and intramolecular domino dearomatisation/spirocyclisation reactions of 2-naphthols.

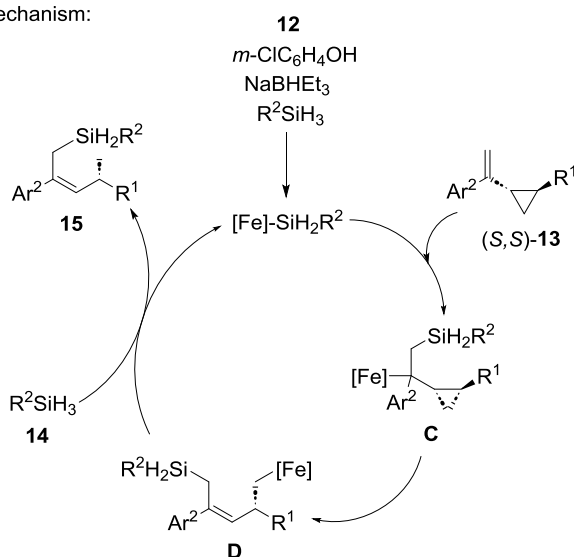
Another type of chiral preformed iron catalyst, namely **12**, was involved by Lu and Hong to perform an asymmetric domino silylation/ring-opening reaction between vinylcyclopropanes **13** and silanes **14** (Scheme 4).¹⁰ In the presence of 5 mol% of catalyst **12** and *meta*-chlorophenol as an additive in dioxane, the process afforded at room temperature within 12-36 hours through anti-Markovnikov selective hydrosilylation chiral allylic silanes **15** with moderate to excellent enantioselectivities (64-99% ee) and moderate yields (37-50%), along with recovered (*R,R*)-**13** with 11-45% yields and 62-99% ee since the process evolved through kinetic resolution. The scope of the one-pot process was found wide as numerous

aryl-substituted vinylcyclopropanes bearing various functional groups at any position on the phenyl ring (Ar) afforded desired products **15** with 92-98% ee and 39-47% yields. The corresponding (*R,R*)-vinylcyclopropanes were recovered with 15-40% yields and 63-97% ee. In contrast, alkyl-substituted vinylcyclopropanes did not react under the same conditions. Moreover, vinylcyclopropanes exhibiting electron-donating or electron-withdrawing groups at the different positions on the phenyl ring at R¹ reacted smoothly to give the products with 40–48% yields and 78-98% ee along with recovered (*R,R*)-vinylcyclopropanes with 13-39% yields and 64-97% ee. The lowest enantioselectivities (64-78% ee) were observed in the reaction of sterically hindered substrates (R¹ = *o*-ClC₆H₄, 2-Naph). To explain the results, the authors proposed the mechanism depicted in Scheme 4 in which an iron-silyl species was generated from **12** in the presence of the silane, *meta*-chlorophenol and NaBHET₃. Then, (*S,S*)-**13** underwent an 1,2-insertion into the iron-silicon bond, producing iron species **C**. Then, the latter underwent a β-carbon elimination to give iron species **D**. A subsequent δ-bond metathesis with the hydrosilane occurred to deliver the final product and regenerated iron silyl species.



$\text{Ar}^2 = p\text{-MeOC}_6\text{H}_4, p\text{-Tol}, p\text{-MeSC}_6\text{H}_4, p\text{-FC}_6\text{H}_4, p\text{-ClC}_6\text{H}_4, p\text{-BrC}_6\text{H}_4, m\text{-Tol}, m\text{-FC}_6\text{H}_4, o\text{-FC}_6\text{H}_4, 2\text{-Naph}, \text{Ph}$
 $\text{R}^1 = p\text{-MeOC}_6\text{H}_4, p\text{-Tol}, p\text{-MeSC}_6\text{H}_4, p\text{-FC}_6\text{H}_4, p\text{-ClC}_6\text{H}_4, p\text{-BrC}_6\text{H}_4, m\text{-FC}_6\text{H}_4, m\text{-ClC}_6\text{H}_4, o\text{-ClC}_6\text{H}_4, 2\text{-Naph}, 1\text{-Naph}, 2\text{-furyl}, 2\text{-thienyl}, n\text{-Pr}, i\text{-Pr}, \text{Cy}, i\text{-Bu}, \text{Ad}$
 $\text{R}^2 = \text{Ph}, p\text{-MeOC}_6\text{H}_4, p\text{-ClC}_6\text{H}_4, o\text{-Tol}, 1\text{-Naph}, \text{Bn}, \text{PhCH=CH}, \text{Bn}(\text{CH}_2)_2, \text{C}_{12}\text{H}_{25}$

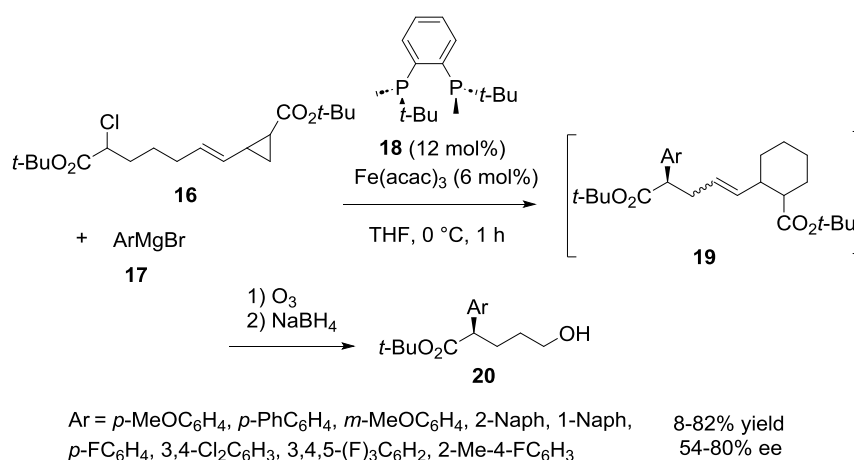
proposed mechanism:



Scheme 4. Domino silylation/ring-opening reaction of vinylcyclopanes with silanes.

In 2020, Gutierrez et al. reported an enantioselective domino radical cyclisation/cross-coupling reaction of vinylcyclopanes **16** exhibiting an α -chloroester group with aryl Grignard reagents **17**, which was promoted by a chiral iron catalyst in situ generated from 6 mol% of $\text{Fe}(\text{acac})_3$ and 12 mol% of chiral bisphosphine ligand **18**.¹¹ The reaction was carried out in THF at 0 °C, thus allowing a mixture of diastereomeric *trans*- and *cis*-products **19** to be

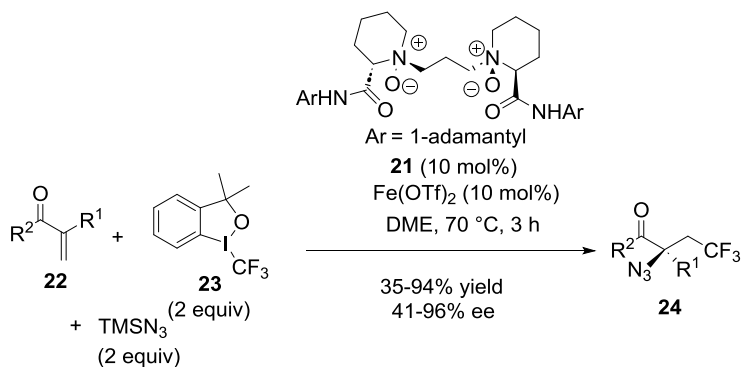
synthesised (Scheme 5). These products were not isolated but directly submitted to ozonolysis followed by reduction with NaBH₄ to give chiral alcohols **20** in 54-80% ee and 8-82% yields. The catalyst system tolerated differently substituted aryl Grignard reagents, including either electron-withdrawing or electron-donating groups. With the aim of expanding the scope of the cascade process, the authors investigated a substrate bearing one more methylene group between the α -chloroester and the vinyl cyclopropane moieties, however, the desired 6-exo-trig radical cyclisation did not occur in this case, probably related to a higher energy barrier to be crossed over in comparison with the 5-exo-trig process.



Scheme 5. Domino radical cyclisation/cross-coupling reaction of vinylcyclopropanes with aryl Grignard reagents followed by ozonolysis and reduction.

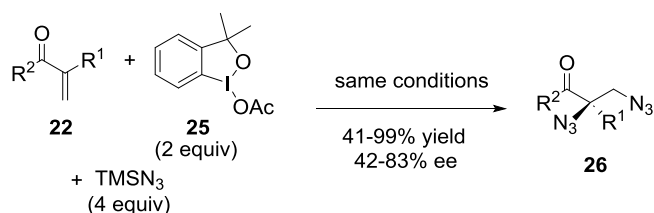
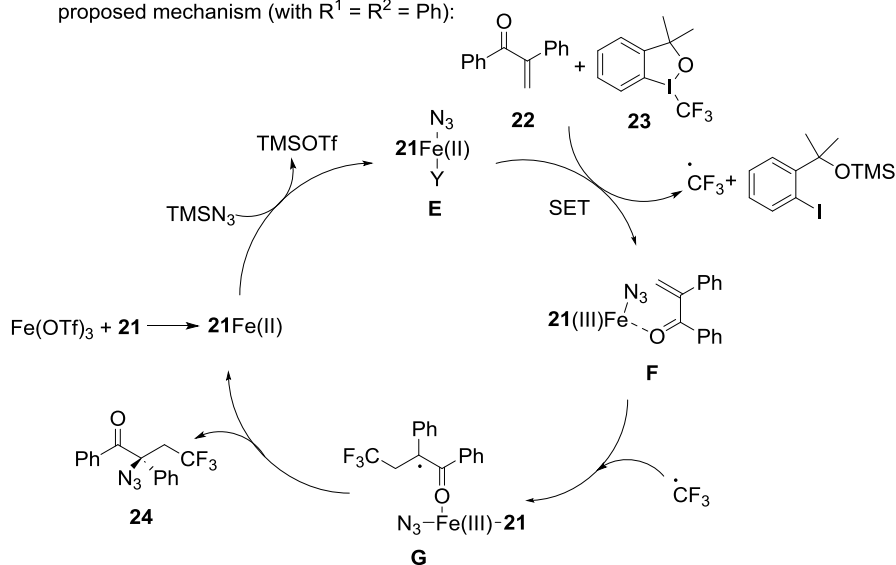
The asymmetric carboazidation of olefins allows a direct access to many chiral halogenated organoazides, constituting precursors of many chiral nitrogen-containing molecules. In 2021, Feng, Liu and Wu developed enantioselective iron-catalysed domino radical carboazidation of α,β -unsaturated ketones performed at 70 °C in DME (Scheme 6).¹² In the presence of 10 mol% of a chiral iron catalyst derived from Fe(OTf)₂ and chiral *N,N'*-dioxide ligand **21**, a range of substituted α,β -unsaturated ketones **22** reacted with radical precursor **23** (2 equiv) and TMSN₃ (2 equiv) as the azide source to give within 3 hours the corresponding chiral α -azido carbonyl derivatives **24** in 41-96% ee and 35-94% yields. A plausible mechanism for this three-component reaction is depicted in Scheme 6, beginning with the formation of iron species **E** from the reaction between the catalyst and TMSN₃. Then, the radical precursor **23** oxidised intermediate **E** via a single-electron transfer (SET) process to generate iron intermediate **F** and CF₃ radical. Subsequently, the latter added to the C=C

bond in species **F** to provide a tertiary radical species **G**. Finally, the latter underwent azido group transfer to give the product along with regenerated catalyst. The same reaction conditions were also applied to the enantioselective radical diazidation of α,β -unsaturated ketones **22** through reaction with TMSN_3 (4 equiv) as the azide source and benziodoxole **25** as the oxidant (2 equiv). In this case, the three-component process resulted in the formation of chiral diazides **26** with 42-83% ee and 41-99% yields, as presented in Scheme 6.



$\text{R}^1 = \text{Ph, } p\text{-MeOC}_6\text{H}_4, o\text{-FC}_6\text{H}_4, o\text{-MeOC}_6\text{H}_4, m\text{-FC}_6\text{H}_4, m\text{-F}_3\text{CC}_6\text{H}_4, m\text{-Tol, } p\text{-Tol}$
 $m\text{-MeOC}_6\text{H}_4, p\text{-FC}_6\text{H}_4, p\text{-ClC}_6\text{H}_4, p\text{-BrC}_6\text{H}_4, p\text{-IC}_6\text{H}_4, p\text{-MeSC}_6\text{H}_4, 3\text{-F-4-MeOC}_6\text{H}_3,$
 $3,4\text{-Cl}_2\text{C}_6\text{H}_3, 2\text{-Naph, 1-Naph, } \text{C}_6\text{H}_4\text{ (1,2- and 1,3-), } \text{C}_6\text{H}_3\text{ (1,2- and 1,3-)}$
 $\text{R}^2 = \text{Ph, } m\text{-ClC}_6\text{H}_4, p\text{-FC}_6\text{H}_4, p\text{-ClC}_6\text{H}_4, p\text{-Tol, } p\text{-MeOC}_6\text{H}_4, 2\text{-thienyl, PhNH}$

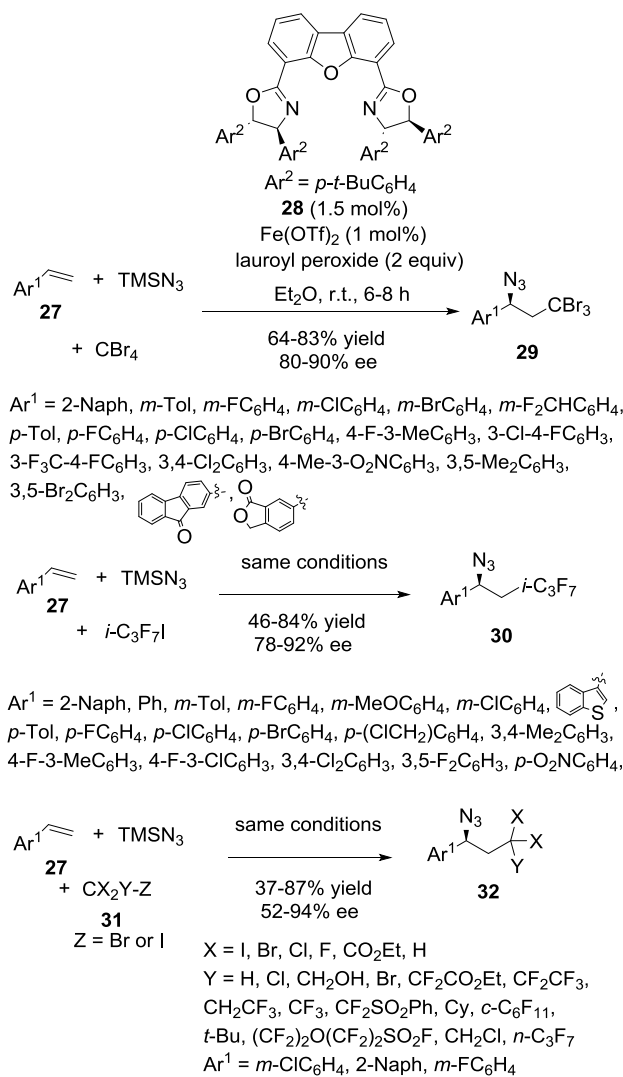
proposed mechanism (with $\text{R}^1 = \text{R}^2 = \text{Ph}$):



$\text{R}^1 = \text{Ph, } o\text{-FC}_6\text{H}_4, o\text{-MeOC}_6\text{H}_4, m\text{-MeOC}_6\text{H}_4, p\text{-BrC}_6\text{H}_4, p\text{-Tol, } p\text{-MeSC}_6\text{H}_4,$
 $p\text{-HOC}_6\text{H}_4, 3,4\text{-Cl}_2\text{C}_6\text{H}_3, 3\text{-F-4-MeOC}_6\text{H}_3, 2\text{-Naph, } \text{C}_6\text{H}_4\text{ (1,2- and 1,3-), } \text{C}_6\text{H}_3\text{ (1,2- and 1,3-)}$
 $\text{R}^2 = \text{Ph, PhNH}$

Scheme 6. Three-component radical carboazidation/diazidation reactions of α,β -unsaturated ketones with radical precursors and TMSN_3 .

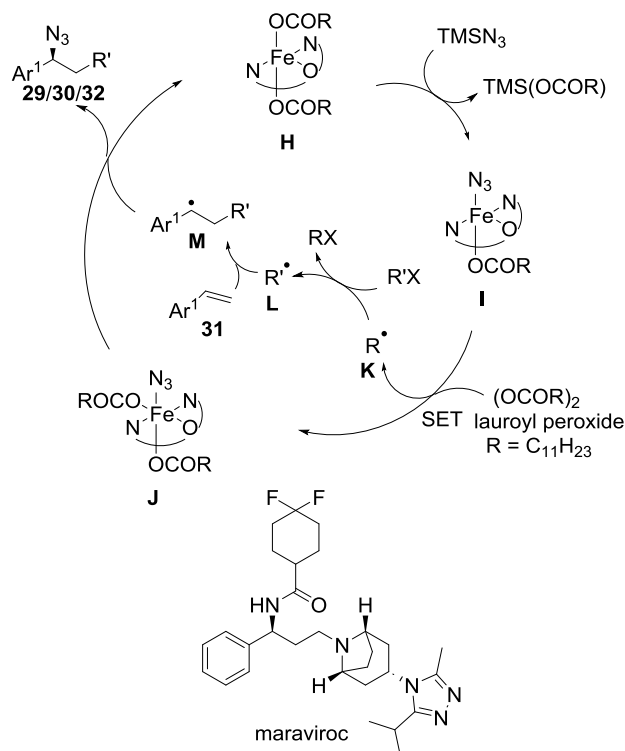
In the same area, Zhang and Bao developed in 2021 a three-component process between styrenes **27**, TMSN₃, and alkyl halides such as CBr₄ (Scheme 7).¹³ It was promoted at room temperature by a chiral iron catalyst in situ generated from only 1 mol% of Fe(OTf)₂ and 1.5 mol% of chiral bisoxazoline ligand **28** in diethylether in the presence of lauryl peroxide as the radical initiator. The domino radical addition/azidation reaction resulted within 6-8 hours in the formation of chiral brominated organoazides **29** in 64-83% yields and 80-90% ee. The catalyst system tolerated styrenes with either electron-withdrawing or electron-donating groups on the phenyl ring. The scope of the reaction was extended to other alkyl halides, such as *i*-C₃F₇I, which provided by reaction with a variety of styrenes and TMSN₃, the corresponding chiral fluorinated products **30** with 46-84% yields and 78-92% ee. Fluoroalkyl bromides or iodides **31** were also compatible substrates, leading to desired products **32** with 37-87% yields and 52-94% ee.



Scheme 7. Three-component carboazidation reactions of styrenes, TMSN_3 and alkyl halides.

The precedent reactions evolved through a carbon radical addition to the $\text{C}=\text{C}$ bond of styrenes followed by an iron-catalysed azido group transfer.¹³ In the mechanism detailed in Scheme 8, initial active catalyst **H** underwent ligand exchange with TMSN_3 to give intermediate **I**. The latter species was then oxidised by lauroyl peroxide via a single electron transfer (SET) to provide azide intermediate **J**. Alkyl radical **K** could abstract iodine atom from starting alkyl iodide to generate alkyl radical **L**, which then added to styrene to form benzylic radical **M**. Subsequently, **J** reacted with **M** to yield the final product. A synthetic utility of this novel procedure was demonstrated in the development of a synthesis of the anti-HIV drug maraviroc.

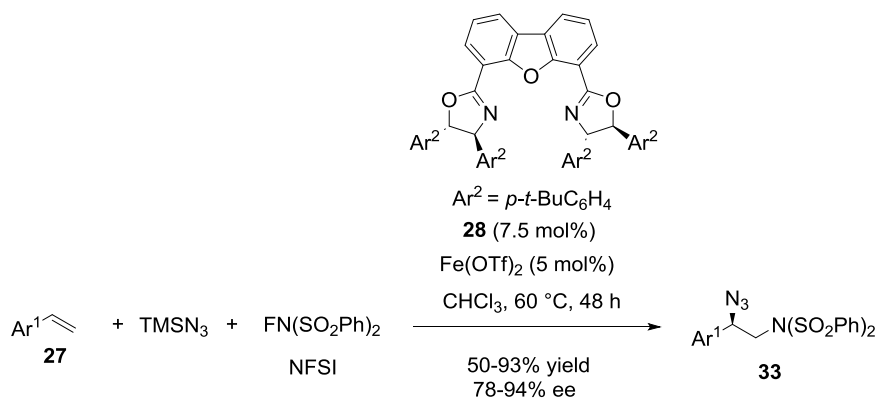
proposed mechanism (with R'X = CBr₄, *i*-C₃F₇I or CX₂Y-Z):



Scheme 8. Mechanism for three-component carboazidation reactions of styrenes, TMSN_3 and alkyl halides.

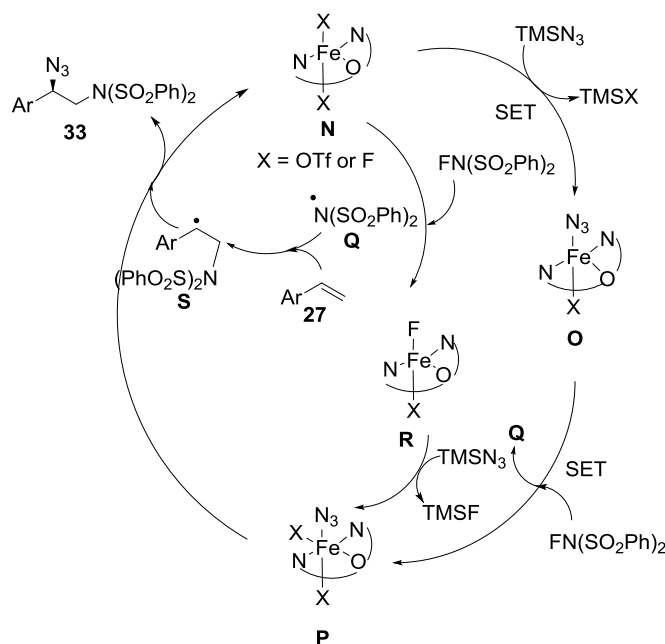
The same authors also developed the first enantioselective radical aminoazidation of styrenes by using the same chiral ligand.¹⁴ The reaction of styrenes **27** with TMSN_3 as the azide source and NFSI as the *N*-radical precursor, promoted at 60 °C in chloroform by a chiral iron catalyst derived from 5 mol% of Fe(OTf)_2 and 7.5 mol% of chiral ligand **28**, resulted within 48 hours in the formation of chiral aminoazides **33** in 50-93% yields and 76-94% ee (Scheme 9). These products constitute potent starting materials to synthesise many useful chiral nitrogenated compounds. The scope of the process was found wide since a range of styrenes exhibiting one or more either electron-donating or electron-withdrawing substituents on the phenyl ring were tolerated, leading to the products with 50-93% yields and 78-94% ee. Moreover, when vinyl and allyl/alkynyl groups ($\text{Ar}^1 = \text{allyl, acetylenyl}$) were present in the same molecule, the aminoazidation occurred selectively at the vinyl group to give the corresponding products with 68-80% yields and 78-80% ee. The lowest enantioselectivity

(76% ee) was observed in the reaction of 2-vinylbenzo[b]thiophene. To explain the results, a mechanism was proposed by the authors (Scheme 9). It involved the formation of iron(II) catalyst **N** which underwent ligand exchange with TMSN_3 to afford iron(II) azide complex **O**. Then, a SET occurred between **O** and NFSI, resulting in the formation of iron(III) azide species **P** along with bis-sulfonylamidyl radical **Q**. Alternatively, the SET process could proceed prior to the ligand exchange with TMSN_3 . Complex **N** participated in a SET with NFSI to afford oxidised iron species **R** and radical **Q** and **R** reacted with TMSN_3 to generate iron(III) azide species **P**. Addition of bis-sulfonylamidyl radical **Q** to the styrene afforded benzyl radical **S**, which could further participate in a group transfer with species **P** to finally lead to the product along with regenerated active catalyst **N**.



$\text{Ar}^1 = m\text{-MeOC}_6\text{H}_4, m\text{-Tol}, m\text{-}i\text{-PrC}_6\text{H}_4, m\text{-OctC}_6\text{H}_4, m\text{-FC}_6\text{H}_4, m\text{-BrC}_6\text{H}_4, m\text{-F}_2\text{HCC}_6\text{H}_4, m\text{-F}_3\text{CC}_6\text{H}_4, 3\text{-Cl-}4\text{-MeC}_6\text{H}_3, 3\text{-Me-}4\text{-FC}_6\text{H}_3, 3,4\text{-F}_2\text{C}_6\text{H}_3, 3\text{-Cl-}4\text{-FC}_6\text{H}_3, 3,4\text{-Cl}_2\text{C}_6\text{H}_3, 3\text{-Me-}4\text{-BrC}_6\text{H}_3, 3\text{-Br-}4\text{-FC}_6\text{H}_3, p\text{-FC}_6\text{H}_4, p\text{-ClC}_6\text{H}_4, p\text{-ClCH}_2\text{C}_6\text{H}_4, p\text{-F}_3\text{CC}_6\text{H}_4, 3\text{-Me-}5\text{-OMe}, 3,5\text{-Me}_2\text{C}_6\text{H}_3, 3,5\text{-F}_2\text{C}_6\text{H}_3, 3,5\text{-Br}_2\text{C}_6\text{H}_3, 3\text{-F-}5\text{-BrC}_6\text{H}_3, 3,5\text{-(F}_3\text{C)}_2\text{C}_6\text{H}_3, 3\text{-F-}4\text{-(allyl)C}_6\text{H}_3, 3\text{-Cl-}4\text{-(HC}\equiv\text{C)C}_6\text{H}_3, \text{thiophene}$

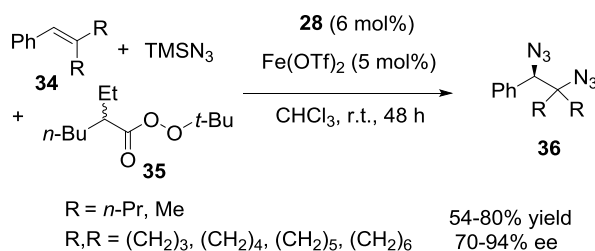
proposed mechanism:



Scheme 9. Three-component aminoazidation of styrenes with TMSN_3 and NFSI.

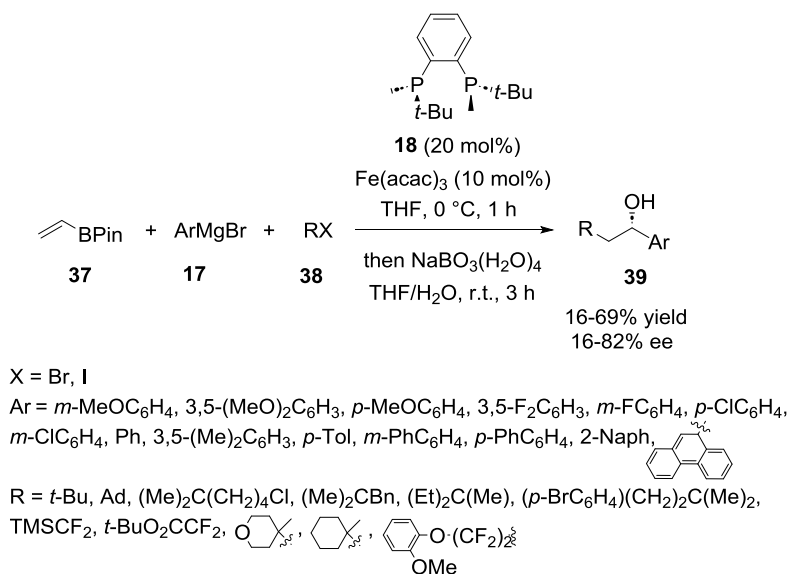
Related reaction conditions were also employed by the same authors to develop the first asymmetric diazidation of trisubstituted styrenes **34** in the presence of TMSN_3 and alkyl perester **35**.¹⁴ In this case, a lower catalyst loading (6 mol%) in ligand **28** was combined with 5 mol% of the same precatalyst $\text{Fe}(\text{OTf})_2$ (Scheme 10). The reaction of a series of

trisubstituted styrenes **34** was performed at room temperature in chloroform, providing the desired otherwise inaccessible chiral diazides **36** in 54-80% yields and 70-94% ee.



Scheme 10. Three-component diazidation of trisubstituted styrenes with TMSN_3 and an alkyl perester.

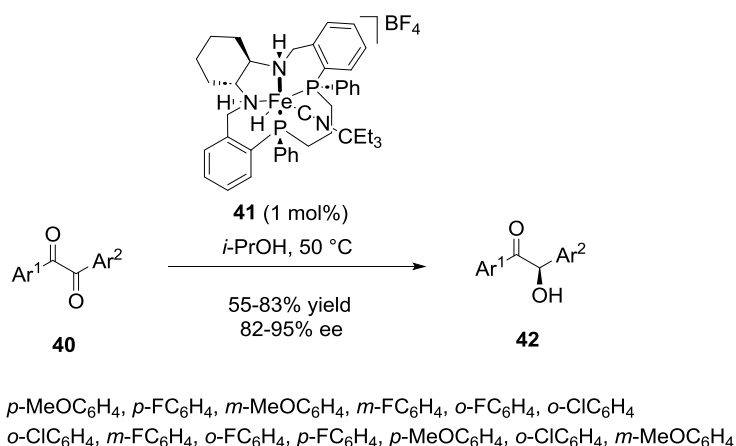
In 2023, chiral bisphosphine ligand **18** was employed by Gutierrez et al. to develop novel regio- and enantioselective three-component cross-coupling reactions between vinyl boronate **37**, (fluoro)alkyl halides **38**, and aryl Grignard reagents **17** (Scheme 11).¹⁵ This practical and simple methodology was performed at 0 °C in THF in the presence of 10 mol% of $\text{Fe}(\text{acac})_3$ and 20 mol% of chiral ligand **18**, allowing the formation of chiral secondary alcohols **39** with 16-69% yields and 26-82% ee within 1 hour after subsequent oxidation. The reaction tolerated both electron-rich and electron-poor aryl Grignard reagents, as well as fluorinated radical precursors. The process evolved through the radical addition of the alkyl halide to the vinyl boronate to give an α -boryl radical, which was subsequently coupled to the aryl Grignard reagent to afford the product.



Scheme 11. Three-component cross-coupling reaction of a vinyl boronate with (fluoro)alkyl halides and aryl Grignard reagents.

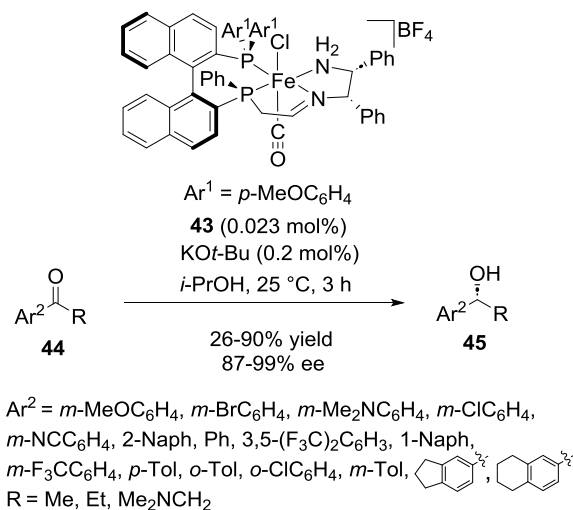
3. Reductions of ketones and imines

Asymmetric reduction of ketones, such as transfer hydrogenation, are commonly catalysed by homogeneous catalysts based on precious toxic metals, such as ruthenium, rhodium or iridium, which present the drawback to be difficult to be removed from the final product. Along these metals, iron represents an inexpensive and environmentally friendly alternative for these reactions since it is abundant and nontoxic. The asymmetric hydrogenation of benzils constitutes the most direct route to chiral benzoin. However, this methodology has not been much developed because it generally involved transition metal-based catalysts requiring activation by a base, which is not compatible with the stereochemical lability of benzoin. To address this issue, Mezzetti and De Luca reported in 2020 the use of novel strictly base-free conditions to perform the asymmetric transfer hydrogenation of benzils **40** with isopropanol as the hydride donor (Scheme 12).¹⁶ The (hemi)hydrogenation was promoted by 1 mol% of preformed chiral N₂P₂ macrocyclic iron(II) hydride complex **41** in isopropanol at 50 °C in the absence of base, thus resulting in the formation of chiral benzoin **42** in 55-83% yields and 82-95% ee. Especially, excellent enantioselectivities (82-94% ee) were obtained in the reaction of challenging *ortho*-substituted substrates.



Scheme 12. Transfer hydrogenation of benzoin derivatives with catalyst **41**.

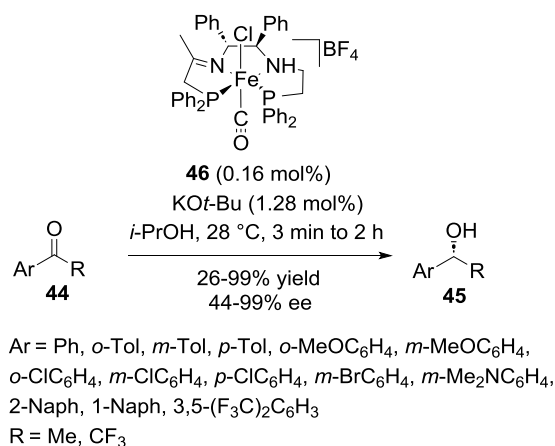
In 2020, Zuo and Wang developed novel iron catalysts including 1,1'-binaphthyl axial chirality, P-centered chirality, and C-centered chirality (Scheme 13).¹⁷ Among them, complex **43** employed at a catalyst loading as low as 0.023 mol% was found the most efficient to promote the asymmetric transfer hydrogenation of variously substituted acetophenones **44** with isopropanol as the hydride donor and solvent, affording within 3 hours chiral alcohols **45** in 26-90% yields and 87-99% ee.



Scheme 13. Transfer hydrogenation of acetophenones with catalyst **43**.

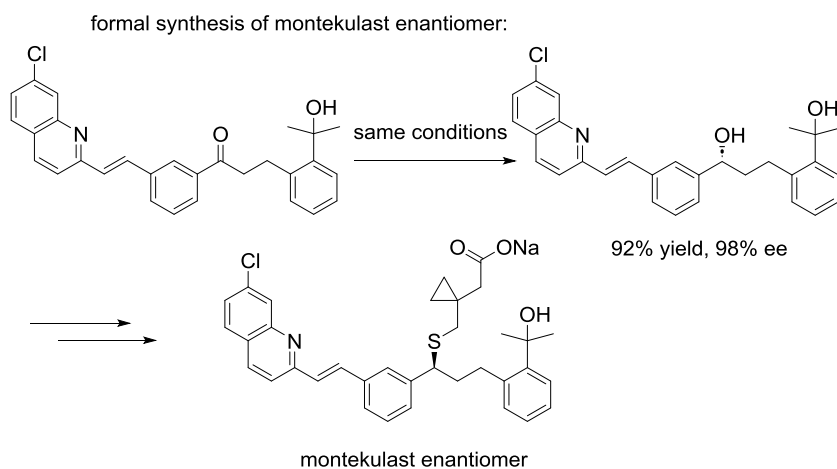
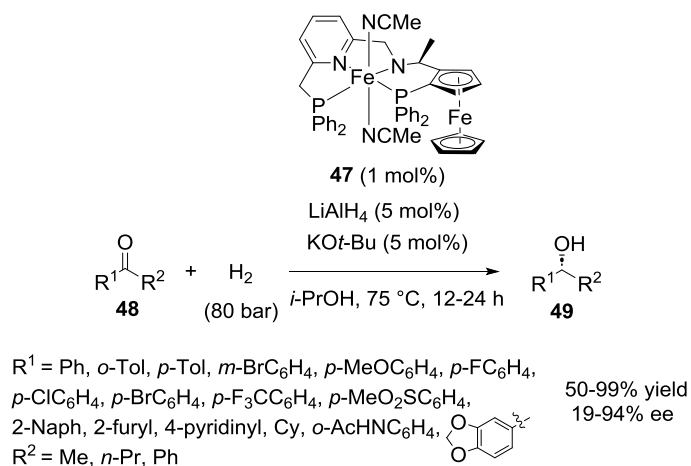
Later in 2021, the same group described the synthesis of other novel chiral amine(imine) diphosphine iron complexes, such as **46** (Scheme 14).¹⁸ They found that only 0.16 mol% of

the latter was sufficient in the presence of a base, such as *t*BuOK, to promote the asymmetric transfer hydrogenation of acetophenones **44** in the presence of isopropanol to give the corresponding chiral alcohols **45** with 26-99% yields and 44-99% ee.



Scheme 14. Transfer hydrogenation of acetophenones with catalyst **46**.

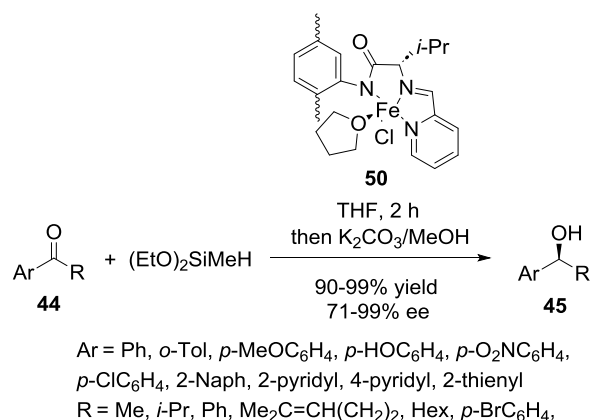
The direct asymmetric hydrogenation of ketones has been widely employed especially in the pharmaceutical industry. Replacing noble metals usually employed in these processes by non-precious metals constitutes a challenge.¹⁹ In 2023, Zhang and Wen designed a novel sterically hindered ferrocene-based tetradentate ligand to be chelated to iron in order to synthesise rigid chiral catalyst **47**.²⁰ This was applied to promote the enantioselective hydrogenation of ketones **48** under hydrogen atmosphere (80 bar) performed at 75 °C in isopropanol as solvent in the presence of LiAlH₄ as hydride donor and *t*-BuOK as base (Scheme 15). Starting from a variety of diaryl and alkyl aryl ketones **48**, various alcohols **49** were synthesised within 12-24 hours with 50-99% yields and 19-94% ee. The poorest results (50% yield, 19% ee) were observed in the reaction of a more challenging dialkyl ketone (R¹ = Cy, R² = Me). This novel catalyst system was employed in a formal synthesis of montelukast which is an antiasthmatic agent.



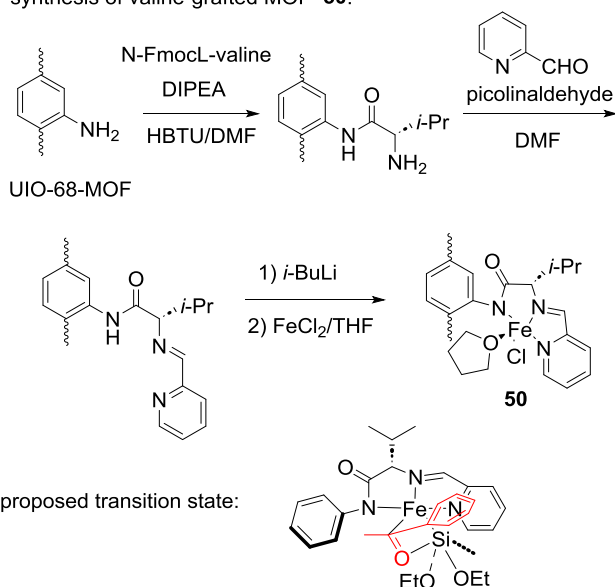
Scheme 15. Hydrogenation of ketones with catalyst **47**.

In comparison with homogeneous catalysts, heterogeneous ones present the advantages to be recyclable and, consequently, more economic. In 2021, Manna and co-workers reported the synthesis of novel highly enantioselective, active and easily tunable heterogeneous iron catalysts based on metal-organic frameworks (MOFs), possessing chiral pores derived from natural amino acids, such as valine, to be used as promoters in the asymmetric hydrosilylation of ketones.²¹ The synthesis of the optimal catalyst **50** derived from L-valine is detailed in Scheme 16. The amino group of UiO-68-MOF was coupled with the carboxylic acid group of L-valine in the presence of hexafluorophosphate benzotriazole tetramethyl uronium (HBTU) and DIPEA in DMF to give the corresponding L-valine-grafted UiO-68-MOF. The latter was then treated with picolinaldehyde and a subsequent metalation with FeCl₂ afforded the final amino acid-functionalised MOFs **50**. This robust heterogeneous catalyst was found efficient in the asymmetric hydrosilylation of ketones **44** with (OEt)₂MeSiH to afford, after

deprotection by treatment with K_2CO_3 in methanol, the corresponding chiral alcohols **45** in 90-99% yields and 90-99% ee. In only one case of substrate ($R^1 = p\text{-BrC}_6\text{H}_4$, $R^2 = \text{Me}$), the reaction provided a lower ee value (76% ee). The catalyst system was compatible to a range of alkyl (hetero)aryl ketones (Scheme 16). It could be readily recycled and reused for more than fifteen times, displaying high turnover numbers of up to 10000. Other catalyst of this type were also developed by the same authors and further applied to the same reactions with comparable results (70-97% yields, 80-99% ee).²² In this case, the heterogeneous catalysts were based on chiral valinol-functionalised metal-organic frameworks (MOFs). To explain the (*S*)-configuration of the product, the authors proposed the transition state detailed in Scheme 16.

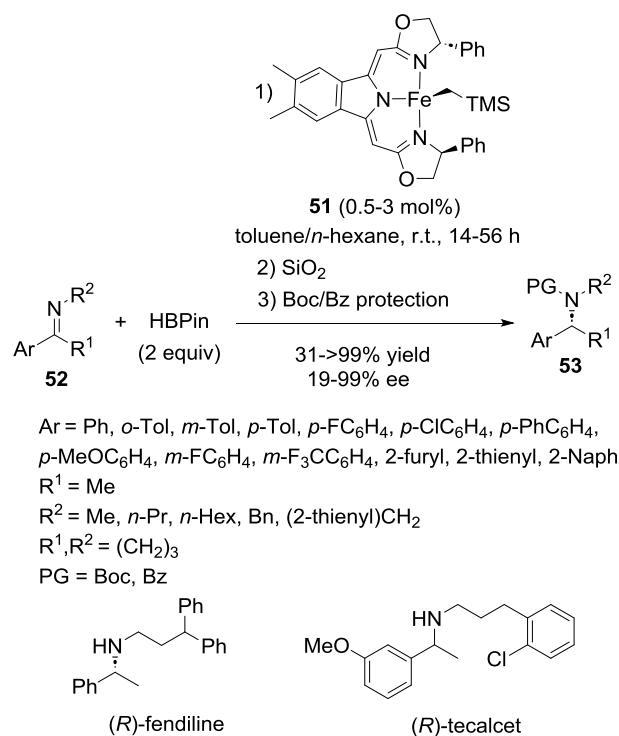


synthesis of valine-grafted MOF **50**:



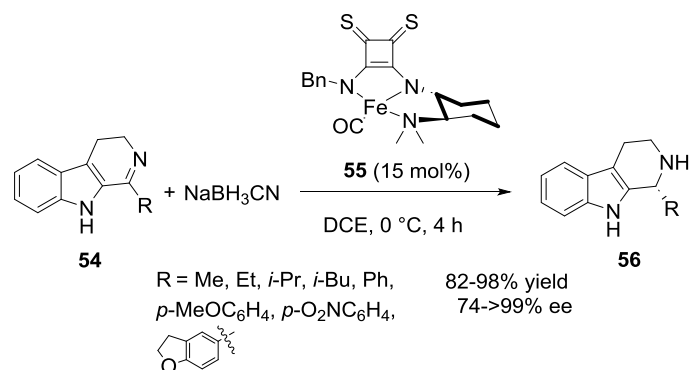
Scheme 16. Hydrosilylation of ketones.

Chiral *N*-alkyl amines constitute key skeletons of many biologically active products. The most direct route to these compounds is based on asymmetric reduction of prochiral imines, which is much less developed in comparison to that of ketones. In 2020, Gade et al. reported the first asymmetric reduction of *N*-alkyl imines promoted by a chiral iron catalyst.²³ To this aim, chiral bis(oxazolinylmethylidene)isoindoline pincer ligands were investigated. Therefore, optimal catalyst **51** was successfully applied to promote the highly enantioselective hydroboration of various *N*-alkyl imines **52** into the corresponding chiral amines **53** in 31->99% yields and 19-99% ee (Scheme 17). It must be noted that a further protection step (PG = Boc or Bz) was performed after the reduction in order to facilitate the isolation and characterisation of the amine product. The process was mostly performed in the presence of 1.5 or 3 mol% of the iron catalyst but in some cases of substrates (Ar = *m*-F₃CC₆H₄), only 0.5 mol% of catalyst loading was sufficient to reach excellent results (99% ee). The catalyst system was compatible with various *para*- and *meta*-substituted *N*-methyl imines which led to the desired amines with high ee values (73->99% ee). On the other hand, the presence of a substituent at the *ortho*-position of the phenyl ring (Ar = *o*-Tol) dramatically affected both reactivity (31% yield) and enantioselectivity (19% ee). Moreover, the reaction of heteroaromatic substrates (Ar = 2-furyl, 2-thienyl) provided lower yields (61-71%) and ee values (32-50% ee). In addition to acyclic *N*-alkyl imines, a cyclic imine (R¹,R² = (CH₂)₃) also reacted smoothly with both high yield (93%) and enantioselectivity (93% ee). Along with *N*-methyl imines (R² = Me), other *N*-alkyl imines with longer alkyl chains (R² = Pr, Hex, Bn, 2-thienylCH₂) were also smoothly reduced with excellent ee values (83->99% ee). The synthetic utility of this procedure was demonstrated in the total synthesis of two drugs, such as the calcium antagonist fendiline used in the treatment of coronary heart disease, and the calcimimetic compound tecalcet employed for the treatment of hyperparathyroidism.



Scheme 17. Hydroboration of *N*-alkyl imines.

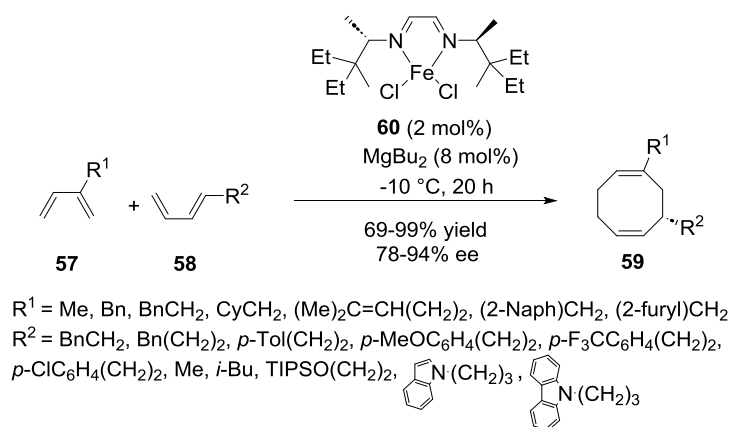
In order to synthesise chiral bioactive tetrahydro- β -carboline, Santos and Nachtigall developed in 2022 an enantioselective imine reduction of dihydro- β -carboline **54** using NaBH₃CN as the reductant agent.²⁴ The methodology employed 15 mol% of chiral thiosquaramide catalyst **55** in DCE at 0 °C, resulting within 4 hours in the synthesis of chiral tetrahydro- β -carboline **56** with 82-98% yields and 74-99% ee (Scheme 18). Either alkyl- or aryl-substituted substrates were compatible but the electronic nature of these substituents were found to affect the enantioselectivity of the reaction. Indeed, while the reaction of the ethyl-substituted substrate provided the desired product with 98% ee, a compound with a branched alkyl substituent (R = *i*-Bu) reacted with a lower ee value (85% ee). Moreover, the reduction of aryl-substituted substrates bearing electronic deficient substituents on the phenyl ring, such as *p*-NO₂-C₆H₄, afforded the products with only 74% ee, whereas aromatic substrates exhibiting an electron-rich substituent, such as *p*-MeO-C₆H₄, reacted with the highest enantioselectivity (99% ee).



Scheme 18. Reduction of dihydro- β -carbolines with NaBH₃CN.

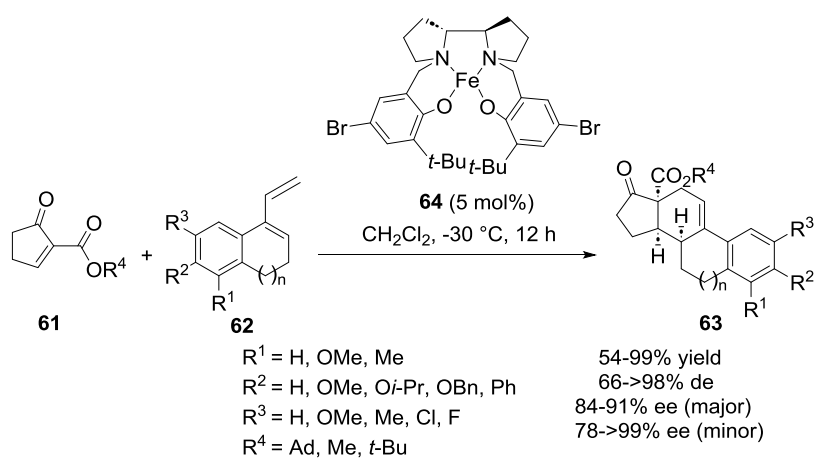
4. Cycloadditions

The asymmetric synthesis of substituted cyclooctadienes still constitutes a challenge in asymmetric iron catalysis in spite of the fact that many naturally occurring bioactive products are based on such skeletons. To fill this gap, Cramer et al. developed in 2020 an enantioselective iron-catalysed enantioselective cross-[4+4]-cycloaddition between 1,3-dienes **57** and **58** to produce chiral disubstituted cyclooctadienes **59**.²⁵ The process occurred at -10 °C within 20 hours in the presence of 2 mol% of chiral α -diimine iron complex **60** activated by 2 mol% of MgBu₂, opening a novel economic and direct access to a wide variety of functionalised cyclooctadienes **59** in 69-99% yields and 78-94% ee (Scheme 19). The catalyst system tolerated a wide variety of linear dienes, including several ones with aryl moieties bearing either electron-donating or electron-withdrawing substituents, which reacted with 75-77% yields and 78-92% ee. Moreover, chiral cyclooctadienes exhibiting various functional groups, such as protected alcohols or carbazole, were synthesised with high enantioselectivity (92% ee). Branched dienes bearing heteroaromatic substituents also reacted smoothly with 80-95% yields and 88-94% ee.



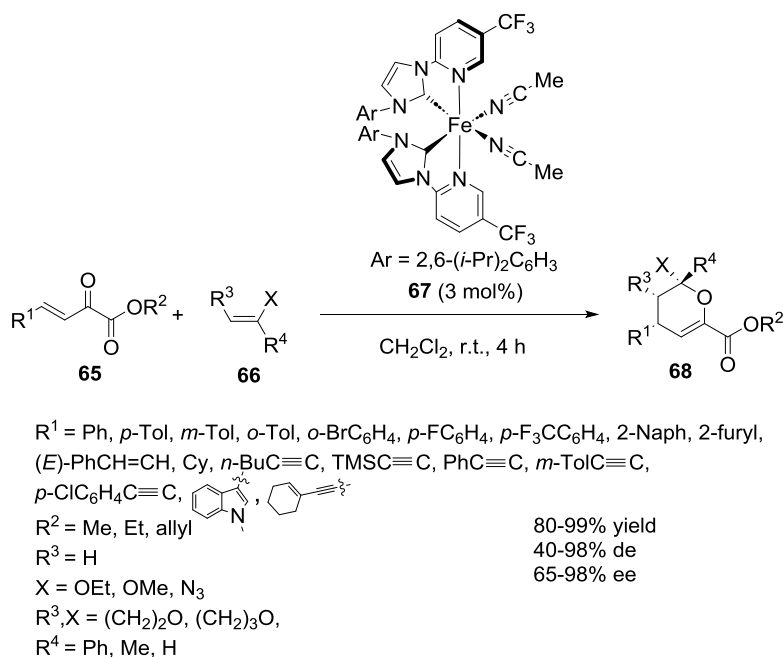
Scheme 19. [4+4] Cycloaddition of 1,3-dienes.

In 2021, Che and Xu described a highly efficient iron-catalysed asymmetric Diels–Alder reaction of various alkylidene β -ketoesters **61** with dienes **62** to afford chiral biologically important estrone analogues **63** (Scheme 20).²⁶ The process required 5 mol% of a chiral BPsalan complex **64** based on a rigid bipyrrolidine backbone and bearing a chiral tetradentate N_2O_2 ligand. Performed at $-30\text{ }^\circ\text{C}$ in dichloromethane, the cycloaddition of vinyl cyclic alkenes **62** with cyclic alkylidene β -ketoesters **61** allowed within 12 hours the formation of a series of differently substituted tetracyclic chiral steroid derivatives **63** with 54-99% yields, 66->98% de, and 78->99% ee for both the two diastereomers generated. It was found that the size of the ester group (R^4) had a great impact on both the diastereo- and enantioselectivities of the reaction. Indeed, methyl esters reacted with much lower ee values (11-39% ee) and diastereoselectivities (66-72% de) than sterically hindered *tert*-butyl or adamantyl esters ($\text{R}^4 = t\text{-Bu, Ad}$) which provided up to >98% de and >99% ee.



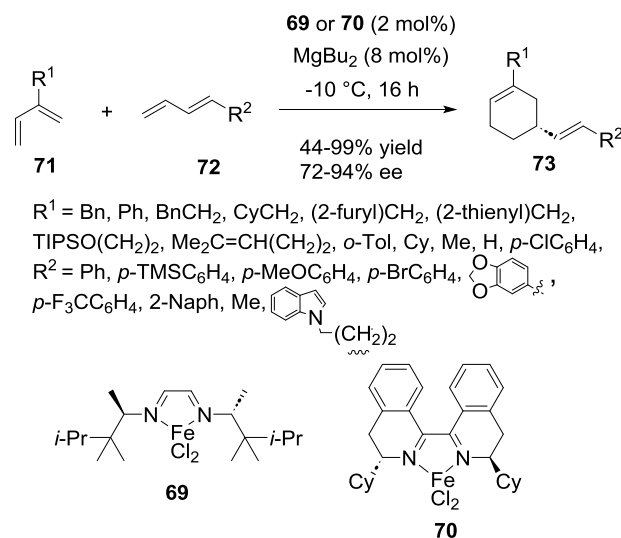
Scheme 20. Diels–Alder reaction of alkylidene β -ketoesters with dienes.

The same year, Meggers et al. demonstrated for the first time that iron complexes exhibiting achiral ligands for which the overall chirality was exclusively due to a stereogenic iron center were capable of catalysing asymmetric hetero-Diels–Alder reactions of β,γ -unsaturated α -ketoesters **65** with enol ethers **66**.²⁷ These catalysts included two configurationally inert achiral bidentate N-(2-pyridyl)-substituted N-heterocyclic carbenes and two labile acetonitriles. Among them, complex **67** bearing bulky 2,6-diisopropylphenyl substituents at the NHC ligands allowed the best enantioselectivities to be reached when employed at room temperature at 3 mol% of catalyst loading (Scheme 21). Indeed, the inverse electron-demand hetero-Diels–Alder reaction of β,γ -unsaturated α -ketoesters **65** as heterodienes with enol ethers **66** as dienophiles performed in dichloromethane as the solvent led within 4 hours to the corresponding chiral 3,4-dihydro-2*H*-pyrans **68** in 80-99% yields with generally excellent diastereo- (40-98% de) and enantioselectivities (65-98% ee). Among dienophiles, 2,3-dihydrofuran ($X, R^3 = O(CH_2)_2$, $R^4 = H$) reacted with a range of variously substituted β,γ -unsaturated α -ketoesters **65** to give chiral bicyclic products **68** in both remarkable diastereo- (>90-98% ee) and enantioselectivities (>90->99% de) combined with high yields (80-99%). The homogeneously excellent results were not affected by the nature of the alkyl ester (R^2). Moreover, different type of substituents (R^1) on the heterodiene was also very well tolerated, spanning from substituted (hetero)aromatic ones to aliphatic, ethylenic, and acetylenic groups. In addition, the reaction of 3,4-dihydro-2*H*-pyran ($X, R^3 = O(CH_2)_3$, $R^4 = H$) with phenyl-substituted β,γ -unsaturated α -keto methylester ($R^1 = Ph$, $R^2 = Me$) afforded the desired bicyclic product in 83% yield, 88% de and 96% ee. Actually, the lowest stereoselectivities (66% de, 65% ee) were observed in the single reaction of 1-methoxyvinylbenzene ($X = OMe$, $R^4 = Ph$) with the same heterodiene, which afforded the corresponding monocyclic cycloadduct in only 40% yield. Along with enol ethers, an 1-azidoethenylbenzene ($X = N_3$, $R^3 = H$, $R^4 = Ph$) could also be used as dienophile, leading to the desired chiral azidopyrane product with both excellent diastereo- (>90% de) and enantioselectivities (95% ee) albeit combined with a moderate yield of 42%.



Scheme 21. Hetero-Diels–Alder reaction of β,γ -unsaturated α -ketoesters with enol ethers/1-azidoethenylbenzene.

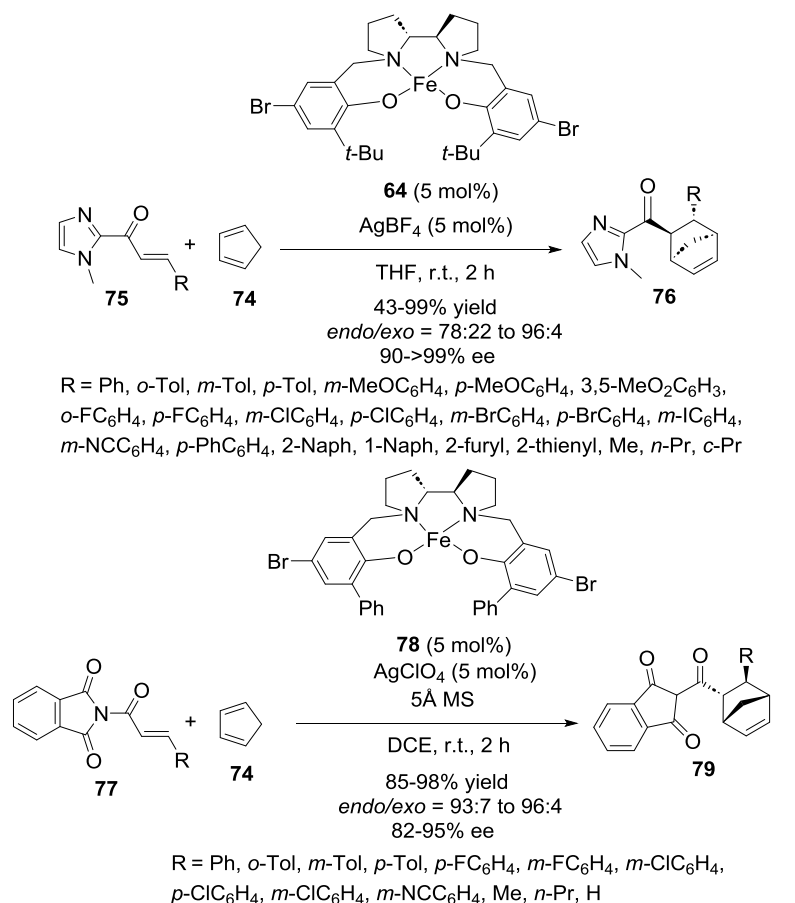
Later in 2022, Cramer and Braconi reported challenging enantioselective iron-catalysed Diels-Alder cycloadditions of unactivated branched and linear dienes performed in the presence of chiral α -diimine preformed iron catalysts **69** and **70**.²⁸ Indeed, the [4+2] cycloaddition of unactivated branched dienes **71** with linear dienes **72** occurred chemo-, regio-, and enantioselectively at $-10\text{ }^\circ\text{C}$ under catalysis with 2 mol% of catalyst **69** or **70** in the presence of MgBu_2 as an additive, leading within 16 hours to the corresponding chiral 1,3-substituted vinyl-cyclohexenes **73** (Scheme 22). The latter were synthesised with 44-99% yields and 72-94% ee. Especially, catalyst **70** derived from a bis-dihydroisoquinoline ligand was found to display a better catalytic performance than catalyst **69** since it allowed the cycloaddition of non-aryl-substituted linear dienes with branched dienes to be achieved, affording the desired chiral cycloadducts with 44-54% yields and 72-92% ee. Moreover, this catalyst also promoted the cycloaddition of simple dienes, such as isoprene ($R^1 = \text{Me}$) or 1,3-butadiene ($R^1 = \text{H}$), with phenyl-substituted linear diene ($R^2 = \text{Ph}$) with high enantioselectivities (92-94% ee) and good yields (53-99%).



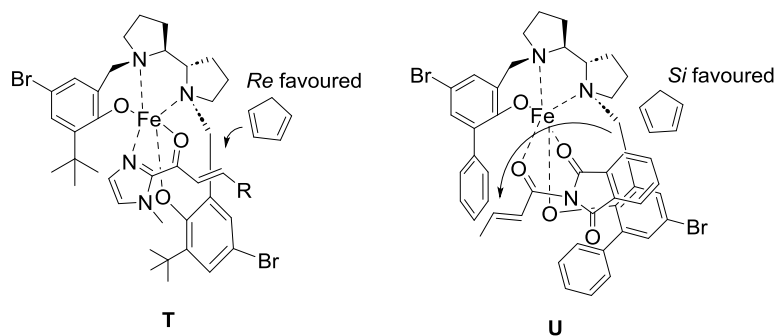
Scheme 22. Diels–Alder reaction of unactivated branched and linear dienes.

Che, Xu and Guo reported in 2022 enantioselective Diels–Alder cycloadditions between cyclopentadiene **74** and α,β -unsaturated acyl imidazoles **75** catalysed by 5 mol% of chiral salan complex **64** (Scheme 23).²⁹ Performed in THF at room temperature in the presence of 5 mol% of AgBF_4 as an additive, the reactions afforded within 2 hours chiral cycloadducts **76** with 43-99% yields combined with generally high *endo*-diastereoselectivities (*endo/exo* = 78:22 to 96:4) and uniformly excellent ee values (90->99% ee). A wide range of either aromatic or aliphatic substituents (R) on the alkene moiety of the α,β -unsaturated acyl imidazole were well tolerated, providing excellent results. However, the reaction of a substrate bearing an *ortho*-fluoro-substituted phenyl group ($\text{R} = o\text{-FC}_6\text{H}_4$) afforded the cycloadduct with the lowest yield (43%) and diastereoselectivity (*endo/exo* = 78:22) combined with a slightly lower ee value (93% ee), which could be related to the steric hindrance effect of the *ortho*-substituted fluorine atom. In a second time, the authors investigated the asymmetric Diels–Alder cycloaddition of cyclopentadiene **74** with more sterically encumbered α,β -unsaturated acyl isoindoline-1,3-diones **77**. In this case, the optimal reaction conditions involved the use at room temperature of 5 mol% of chiral salan catalyst **78** combined with 5 mol% of AgClO_4 in DCE as solvent, to give chiral cycloadducts **79** bearing an opposite absolute configuration. A range of variously substituted products were synthesised with 85-98% yields combined with both high *endo*-diastereoselectivities (*endo/exo* = 93:7 to 96:4) and enantioselectivities (82-95% ee), as shown in Scheme 23. The fact that the absolute structures of the corresponding cycloadducts arisen from α,β -unsaturated 2-acyl imidazoles and α,β -unsaturated acyl isoindoline-1,3-diones catalysed by the same type

of iron salan complexes were opposite could be attributed to the different coordination mode, thus providing an easy method to access to both enantiomers. The authors proposed the two transition states depicted in Scheme 23 to explain these results. The cationic iron salan complex of **64** activated the imidazole through coordination to give intermediate **T**, in which the *Si* face was sterically hindered by the *tert*-butyl group of the ligand, thus favoring the attack of the cyclopentadiene from the *Re* face. Similarly, intermediate **U** was formed upon coordination of the cationic complex of **78** with isoindolinedione **77**. However, due to the more bulky isoindolinedione moiety in comparison with that of the imidazole in **75**, the coordination mode was inversed in **U**, avoiding the repulsion between isoindolinedione and the phenyl substituent of **78**. The *Re* face in **U** being blocked by the phenyl group of **78** made the cycloadduct formed with the inversed absolute configuration.



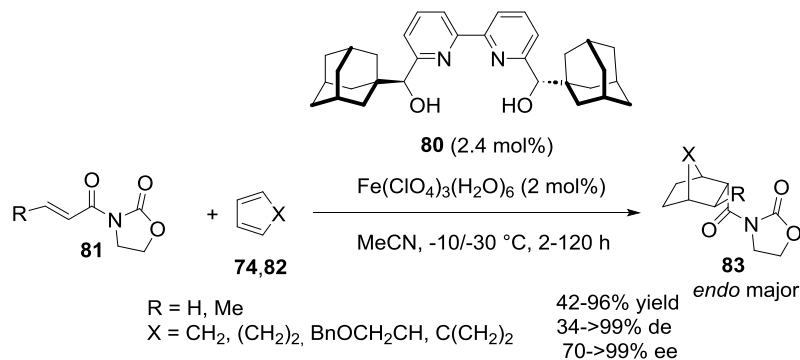
proposed transition states:



Scheme 23. Diels–Alder reactions of cyclopentadiene with α,β -unsaturated acyl imidazoles and α,β -unsaturated acyl isoindoline-1,3-diones.

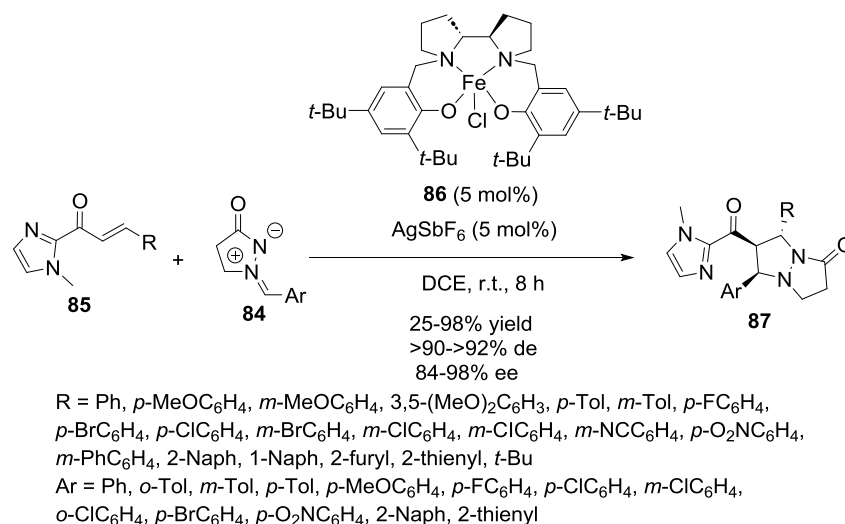
In the same year, Ollevier et al. disclosed the synthesis of novel chiral 2,2'-bipyridine- α,α' -1-adamantyl-diyl ligand **80** (Scheme 24).³⁰ This bulky ligand was investigated in asymmetric iron-catalysed Diels–Alder cycloaddition between α,β -unsaturated oxazolidin-2-ones **81** and various cyclic dienes **74,82**. When employed at 2.4 mol% of catalyst loading in combination

with 2 mol% of $\text{Fe}(\text{ClO}_4)_3 \cdot 6\text{H}_2\text{O}$ as precatalyst in acetonitrile as solvent, the reaction afforded chiral cycloadducts **83** major *endo*-diastereomers with moderate to excellent yields (42-96%), diastereo-(34->99% de), and enantioselectivities (70->99% ee).



Scheme 24. Diels–Alder reaction of α,β -unsaturated oxazolidin-2-ones with cyclic dienes.

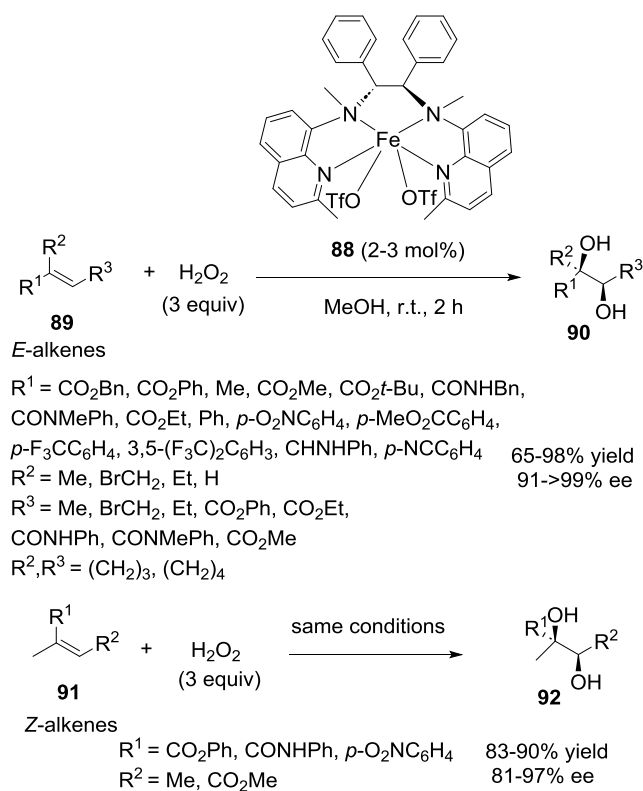
In 2023, Xu and Che reported an efficient enantioselective iron-catalysed [3+2] cycloaddition of *N,N'*-cyclic azomethine imines **84** with α,β -unsaturated acyl imidazoles **85**.³¹ Among several chiral iron salan catalysts investigated, complex **86** exhibiting sterically encumbered *tert*-butyl groups was selected as optimal preformed catalyst to promote the cycloaddition at room temperature (Scheme 25). Employed at 5 mol% of catalyst loading in the presence of the same quantity of AgSbF_6 as an additive in DCE as the solvent, complex **86** promoted the reaction of azomethine imines **84** with variously substituted α,β -unsaturated acyl imidazoles **85** to give within 8 hours chiral biologically interesting *N,N'*-bicyclic pyrazolidines **87** bearing three contiguous stereocenters with 25-98% yields, as almost single diastereomers (>90->92% de) and uniformly high enantioselectivities (84-98% ee). The catalyst system tolerated a wide range of aryl-substituted α,β -unsaturated acyl imidazoles bearing either electron-donating or electron-withdrawing substituents on the phenyl ring. Interestingly, substrates with heteroaromatic substituents (R = 2-furyl, 2-thienyl) were also compatible, leading to products with high diastereo- (>90->92% de) and enantioselectivities (88-94% ee) albeit combined with lower yields (25-33%), which could be related to the strongly electron-donating character of these heterocycles. Furthermore, the scope of the reaction could be extended to an alkyl-substituted α,β -unsaturated acyl imidazole (R = *t*-Bu), which afforded the desired cycloadduct with a moderate yield (57%) but with excellent stereoselectivities (>90% de, 95% ee).



Scheme 25. [3+2] Cycloaddition of *N,N'*-cyclic azomethine imines with α,β -unsaturated acyl imidazoles.

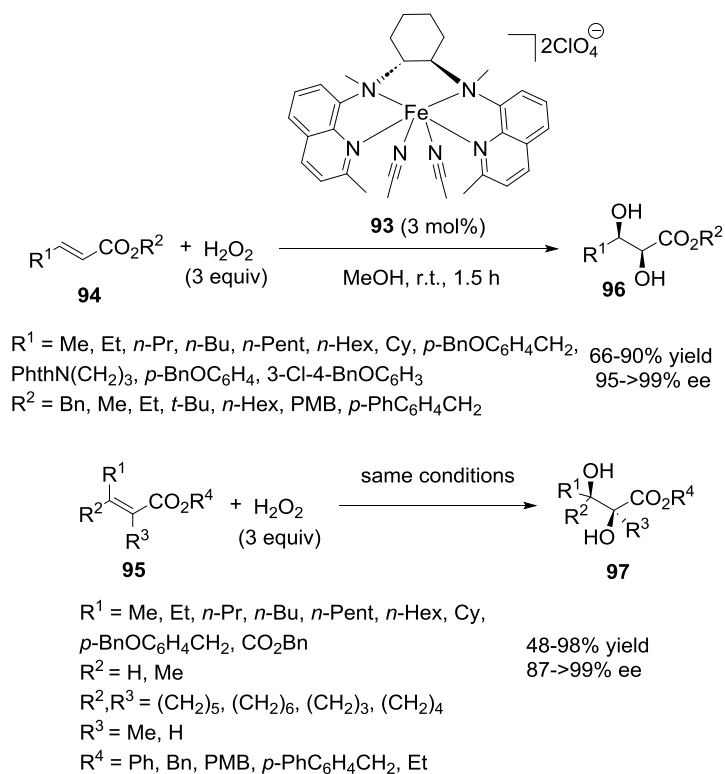
5. Additions to alkenes

The asymmetric *cis*-dihydroxylation of trisubstituted alkenes allow the formation of chiral *cis*-diols exhibiting a quaternary stereogenic center. These compounds are present in many biologically active products and also constitute key building blocks in synthetic organic chemistry. In 2020, Che et al. developed a novel and green methodology to prepare these molecules under mild reaction conditions.³² Indeed, aqueous H₂O₂ was employed as benign oxidant in methanol at room temperature. The reaction was promoted by 2-3 mol% of novel chiral iron catalyst **88** derived from a tetradentate BQPN-type ligand (BQPN = *N,N'*-bis(quinolin-8-yl)-1,2-diphenyl-ethane-1,2-diamine). Under these conditions, a range of (*E*)-trisubstituted alkenes **89** were converted within 2 hours into chiral *cis*-diols **90** in 65-98% yields and 91->99% ee (Scheme 26). Aliphatic as well as aromatic (*E*)-alkenes bearing electron-withdrawing substituents, such as esters and amide groups, were especially well tolerated. Furthermore, the scope of the methodology was applicable to (*Z*)-trisubstituted alkenes **91** which produced the corresponding chiral *cis*-diols **92** with both high yields (83-90%) and enantioselectivities (81-97% ee), as shown in Scheme 26.



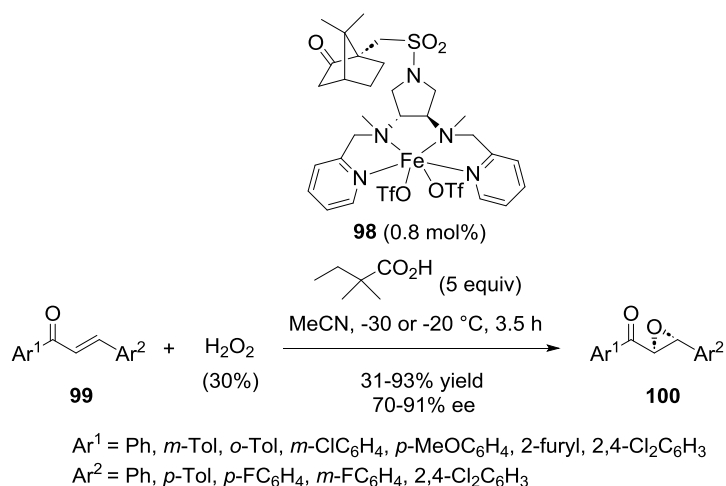
Scheme 26. *Cis*-Dihydroxylations of (*Z*)- and (*E*)-trisubstituted alkenes.

In 2022, Wang and Nam designed related chiral catalysts to be investigated in comparable *cis*-dihydroxylation reactions of multisubstituted aliphatic acrylates with H₂O₂ (Scheme 27).³³ Using 3 mol% of optimal catalyst **93** in methanol at room temperature allowed the chemo- and enantioselective *cis*-dihydroxylation of variously substituted acrylates **94,95** within 1.5 hour with 48-98% yields and 87->99% ee. Especially, the reaction of a range of β-alkyl/aryl-substituted acrylates **94** afforded chiral *syn*-diols **96** with 66-90% yields and 95->99% ee and that of α,β- and β,β-dialkyl-substituted acrylates **95** gave products **97** with 48-98% yields and 87->99% ee.



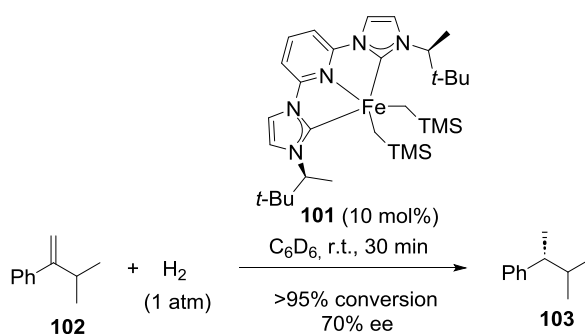
Scheme 27. *Cis*-Dihydroxylations of β -alkyl/aryl-, α,β -dialkyl-, and β,β -dialkyl-substituted acrylates.

Epoxides are strained three-membered rings of wide importance as versatile synthetic intermediates in the total synthesis of numerous important products.³⁴ In 2020, Zhao et al. reported the synthesis of novel chiral tetradentate ligands to be employed in asymmetric iron-catalysed epoxidation of α,β -unsaturated ketones with H_2O_2 .³⁵ These ligands including a diaminopyrrolidine moiety were coordinated with iron to synthesise preformed chiral non-heme iron complexes. Among them, catalyst **98** employed at only 0.8 mol% of catalyst loading in acetonitrile in the presence of H_2O_2 and 2,2-dimethylbutyric acid as an additive allowed the enantioselective epoxidation of various α,β -unsaturated ketones **99** into chiral epoxides **100** to be achieved in 31-93% yields and 70-91% ee (Scheme 28). In general, the ee values were found high ($\geq 80\%$ ee) excepted in the reaction of an heterocyclic-substituted chalcone ($\text{Ar}^2 = 2\text{-furyl}$) which provided only 72% ee.



Scheme 28. Epoxidation of chalcones.

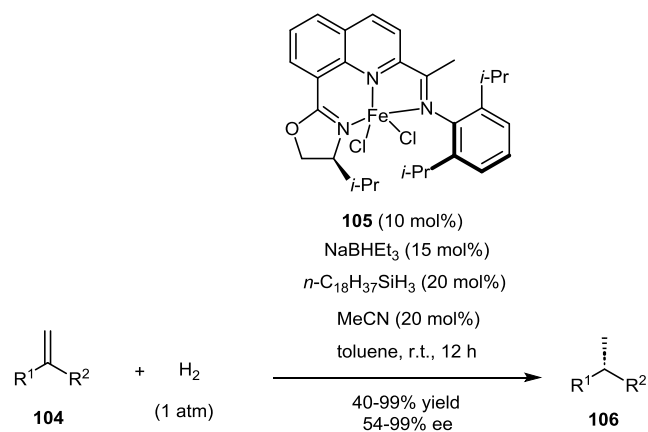
In another area, novel *N*-alkyl-imidazole-substituted pyridine dicarbene iron dialkyl complexes were designed by Chirik et al. in 2021 to be further investigated as promoters in the asymmetric hydrogenation of alkenes.³⁶ Among them, chiral catalyst **101** employed at 10 mol% of catalyst loading at room temperature provided the best result in the asymmetric hydrogenation of alkene **102** into enantiomerically enriched product **103** (Scheme 29). In spite of a high activity (>95% conversion), the enantioselectivity of the reaction was found moderate (70% ee).



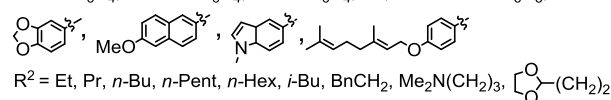
Scheme 29. Hydrogenation of an alkene.

Lu et al. reported the same year highly enantioselective hydrogenation of a wide range of 1,1-disubstituted alkenes **104**.³⁷ The reaction was performed at room temperature under of hydrogen atmosphere (1 atm) in toluene as solvent in the presence of NaBHET_3 , $n\text{-C}_{18}\text{H}_{37}\text{SiH}_3$ and acetonitrile as additives, along with 5 mol% of chiral iron catalyst **105** derived from a

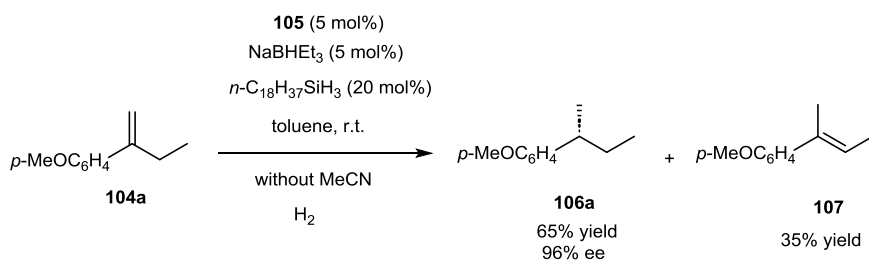
chiral 8-oxazoline iminoquinoline ligand (Scheme 30). It resulted in the formation of a range of chiral alkanes **106** with 40-99% yields and 54-99% ee within 12 hours. In addition to (hetero)aromatic alkenes which provided generally high ee values (70-99% ee), a more challenging dialkyl substrate ($R^1 = p\text{-MeOC}_6\text{H}_4(\text{CH}_2)_2$, $R^2 = i\text{-Pr}$) could also be hydrogenated albeit with both lower yield (40%) and enantioselectivity (54% ee). In this study, the use of acetonitrile as an additive allowed a high chemical selectivity to be achieved by inhibiting the isomerization side-reaction. Indeed, when the hydrogenation of an 1,1-disubstituted alkene **104a** ($R^1 = p\text{-MeOC}_6\text{H}_4$, $R^2 = \text{Et}$) was performed in the absence of acetonitrile, it led to the formation of 35% of the isomerized trisubstituted alkene **107** along with expected hydrogenated product **106a** (Scheme 30). The authors proposed the mechanism depicted in this Scheme, beginning with the generation of an iron hydride species **V** in the presence of NaBHET_3 . Subsequent coordination of the olefin followed by insertion produced iron alkyl species **W**. The latter underwent σ -bond metathesis with the hydrosilane to afford the chiral alkane product along with iron silyl species **X**, which reacted with H_2 to regenerate the iron hydride species **V** via σ -bond metathesis. The role of acetonitrile as an additive might be to prevent the 2,1-insertion as well as to inhibit the β -hydride elimination of iron intermediate via 2,1-insertion to produce the undesired isomerized trisubstituted alkene **107**.



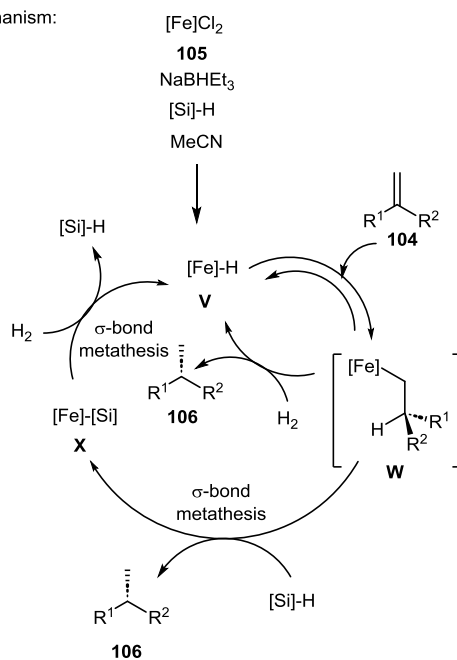
R¹ = *p*-MeOC₆H₄, *p*-BnOC₆H₄, *p*-TBSOC₆H₄, *p*-Tol, *p*-Me₂NC₆H₄,
p-MeSC₆H₄, *p*-PinBC₆H₄, *p*-FC₆H₄, *p*-ClC₆H₄, *p*-BrC₆H₄, *p*-MeOC₆H₄(CH₂)₂,
m-MeOC₆H₄, *m*-TBSOC₆H₄, *o*-MeOC₆H₄, Ph, 3-MeO-4-MeC₆H₃,



role of MeCN as additive:

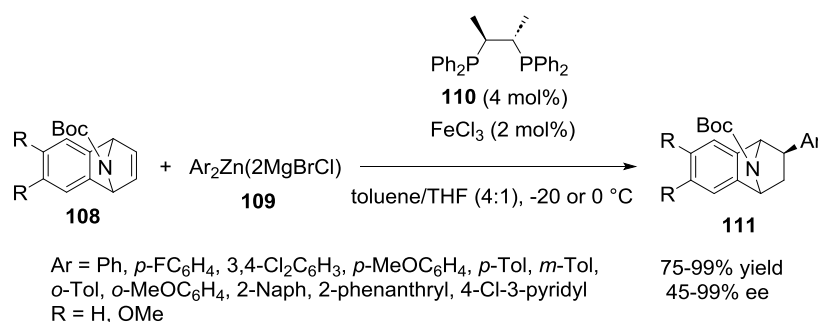


proposed mechanism:



Scheme 30. Hydrogenation of 1,1-disubstituted alkenes.

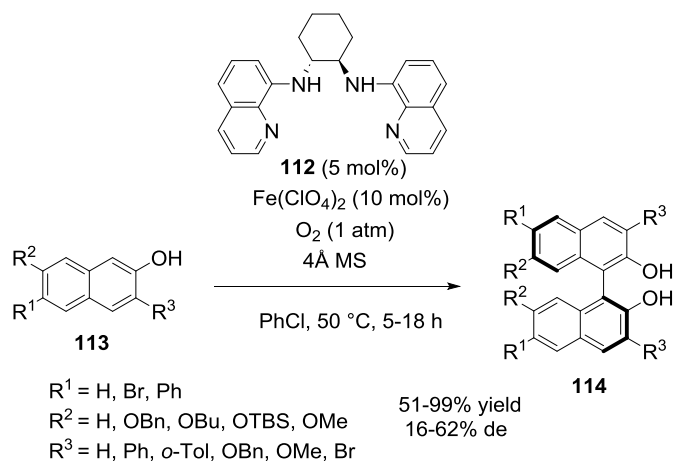
The first enantioselective carbometalation reaction between azabicycloalkenes **108** and arylzinc reagents **109** was disclosed in 2021 by Nakamura and Isozaki by involving an asymmetric iron catalysis.³⁸ The catalyst was in situ generated from 2 mol% of FeCl₃ and 4 mol% of chiral bisphosphine ligand **110** in a 4:1 mixture of toluene and THF as the solvent. As presented in Scheme 31, the reaction performed at -20 or 0 °C afforded chiral bicyclic products **111** in 75-99% yields and 45-99% ee.



Scheme 31. Carbometalation reaction of azabicycloalkenes with arylzinc reagents.

6. Coupling reactions

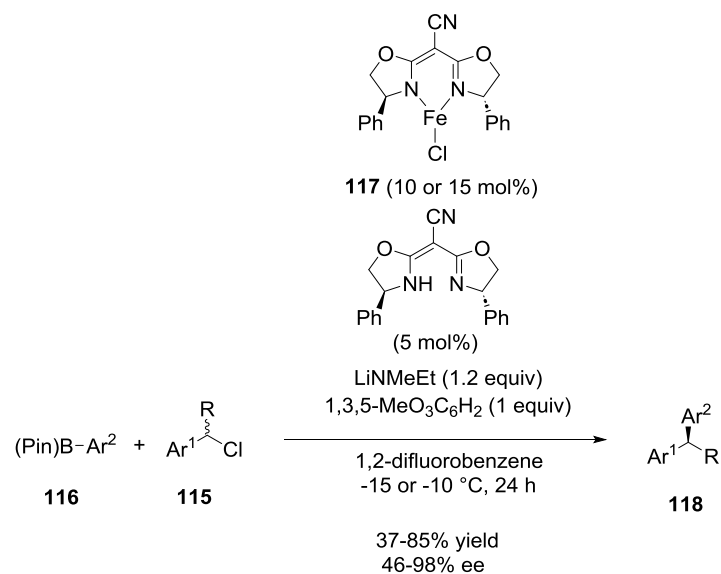
Enantioselective transition-metal-catalysed cross-coupling reactions of alkyl electrophiles with organometallic reagents constitute powerful tools for the construction of carbon–carbon bonds.³⁹ In this context, the transition-metal-catalysed asymmetric oxidative coupling of 2-naphthols represents the simplest methodology to prepare chiral BINOL derivatives. In a recent and rare example, Liu et al. employed a chiral iron complex in situ generated from 10 mol% of Fe(ClO₄)₂ and 5 mol% of chiral bisquinolyldiamine **112** to promote at 50 °C in chlorobenzene as the solvent the asymmetric oxidative coupling of a range of variously substituted 2-naphthols **113** (Scheme 32).⁴⁰ Performed under oxygen atmosphere (1 atm) as the oxidant, the coupling resulted within 5-18 hours in the formation of the chiral BINOL derivatives **114** in 51-99% yields and 16-62% de.



Scheme 32. Oxidative coupling reaction of 2-naphthols.

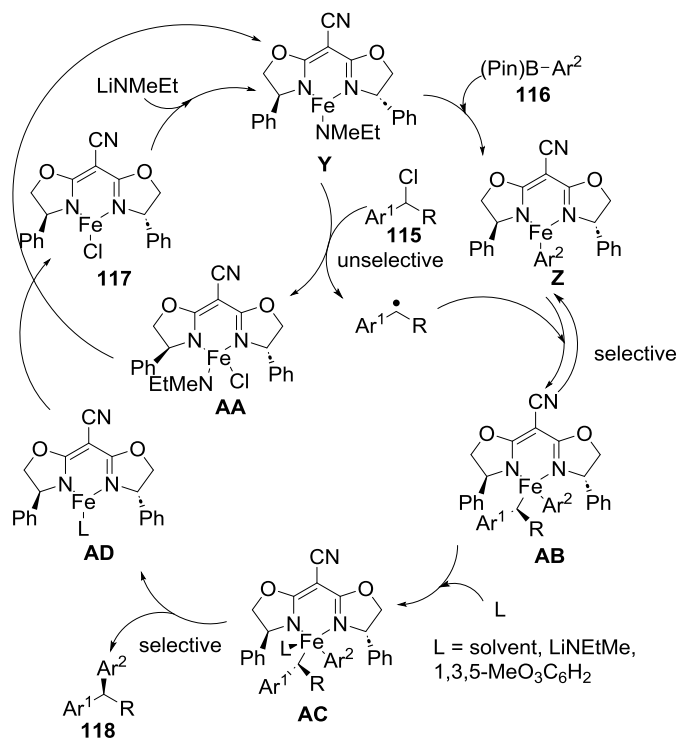
In 2020, Tyrol et al. described the first enantioselective iron-catalysed Suzuki–Miyaura cross-coupling reaction between benzylic chlorides **115** and unactivated arylboronic-pinacol esters **116** (Scheme 33).⁴¹ The process was performed at -15 or -10 °C in *ortho*-difluorobenzene as the solvent in the presence of 10 or 15 mol% of preformed iron catalyst **117** including a chiral cyanobis(oxazoline) ligand. Using LiNMeEt as a base and 1,3,5-trimethoxybenzene as a stoichiometric additive, the process led within 24 hours to chiral 1,1-diarylalkanes **118** with 37-85% yields and 46-98% ee. A series of benzyl chlorides was tolerated but the presence of electron-donating and electron-withdrawing substituents on the phenyl ring led generally to lower yields (40-63%) and enantioselectivities (54-66% ee). Increasing the chain length of the alkyl substituent (R) from methyl to butyl group provided slightly lower yields and comparable ee values while introducing a branching alkyl group adjacent to the alkyl halide resulted in both lower yield and enantioselectivity. Noteworthy, especially high enantioselectivities (86-90% ee) were observed for challenging benzylic halides containing *ortho*-substituted aryl groups. These products are important because *ortho*-substituted 1,1-diaryl alkanes constitute the skeleton of many drugs. Concerning the arylboronic acid pinacol esters, coupling partners derived from 2-phenylboronic acid pinacol ester ($\text{Ar}^2 = \text{phenyl}$) were found less reactive than 2-naphthylboronic acid pinacol ester ($\text{Ar}^2 = 2\text{-Naph}$). Consequently, reactions involving these nucleophiles required both higher temperatures (-10 °C vs -15 °C) and catalyst loadings (15 vs 10 mol%) to provide useful yields. The authors proposed a mechanism which is depicted in Scheme 33. It proposed that catalyst **117** reacted with LiNMeEt to form amide intermediate **Y**. The latter underwent transmetalation with the aryl boronic ester to form aryl intermediate **Z** and unselective

halogen abstraction to form amide-halide **AA** along with a carbon-centered radical. The latter reversibly recombined with intermediate **Z** to give aryl alkyl species **AB**, which was stabilised through coordination with the solvent or 1,3,5-trimethoxybenzene into intermediate **AC**. This complex subsequently underwent reductive elimination to generate intermediate **AD** along with the final cross-coupled product. Then, intermediate **AD** reacted with intermediate **AA** to complete the catalytic cycle by regenerating catalyst **117** and intermediate **Y**.



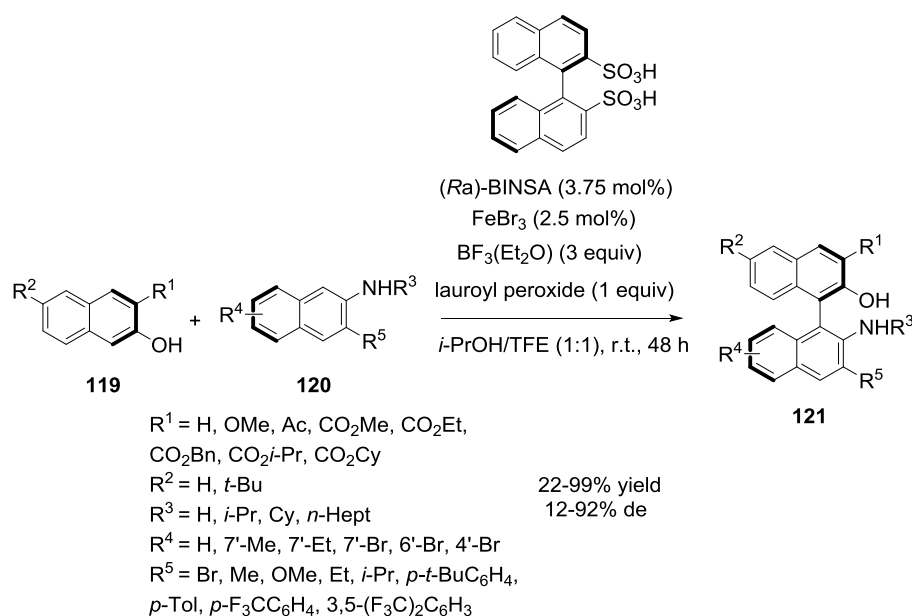
$Ar^1 = Ph, p\text{-Tol}, p\text{-FC}_6\text{H}_4, p\text{-TBSOC}_6\text{H}_4, o\text{-ClC}_6\text{H}_4, o\text{-Tol}, m\text{-BrC}_6\text{H}_4, 2\text{-Naph}$
 $Ar^2 = 2\text{-Naph}, p\text{-Tol}, p\text{-MeOC}_6\text{H}_4, m\text{-F}_3\text{CC}_6\text{H}_4, p\text{-}t\text{-BuC}_6\text{H}_4, Ph$
 $R = Me, Et, n\text{-Pr}, n\text{-Bu}, i\text{-Pr}$

proposed mechanism:



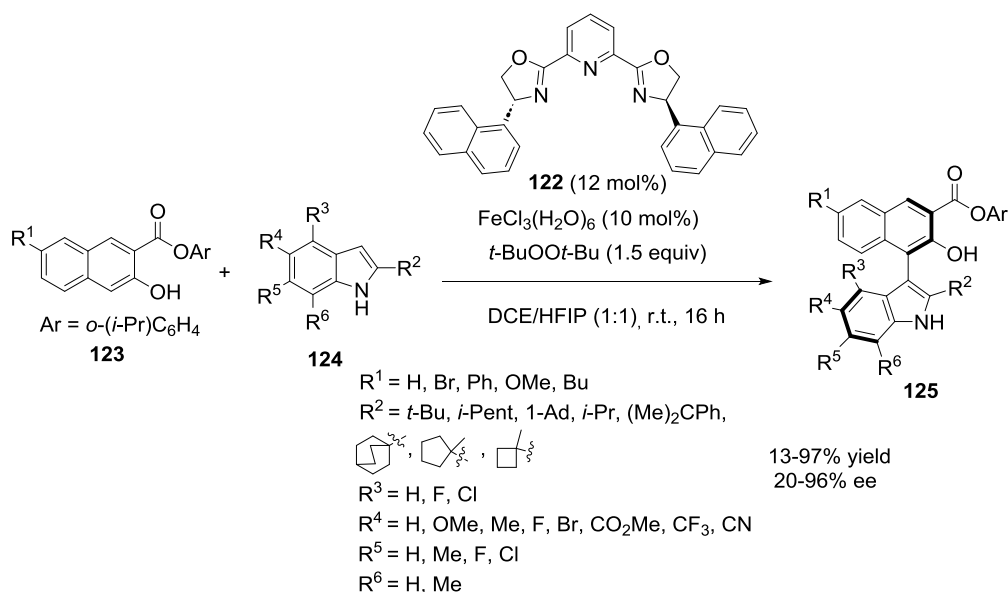
Scheme 33. Suzuki–Miyaura cross-coupling reaction of benzylic chlorides with arylboronic pinacol esters.

In 2022, Pappo et al. developed novel chiral redox disulfonate iron complexes to be applied in enantioselective oxidative cross-coupling reactions between 2-naphthols **119** and 2-aminonaphthalenes **120** (Scheme 34).⁴² Among these complexes, the chiral catalyst in situ generated from 2.5 mol% of FeBr₃ and 3.75 mol% of chiral disulfonic acid ligand (*Ra*)-BINSAs was found optimal when employed at room temperature in a 1:1 mixture of isopropanol and 2,2,2-trifluoroethanol (TFE) as the solvent. The coupling reaction was performed in the presence of lauroyl peroxide (1 equivalent) as the oxidant and BF₃·Et₂O (3 equivalents), resulting within 48 hours in the formation of a wide range of chiral polysubstituted (*Ra*)-2-amino-2'-hydroxy-1,1'-binaphthyls **121** with 25-99% yields and 12-92% ee. Studying the scope of the reaction, the authors found that the presence of a chelating group, such as an ester group, at the 3-position (R¹) of the 2-naphthol was found essential for achieving high enantioselectivity. Moreover, the presence of a *t*-butyl group in R² improved the reactivity of the reaction. For example, the coupling of unsubstituted 2-naphthol (R¹ = R² = H) with 2-aminonaphthalene (R³ = R⁴ = R⁵ = H) led to the corresponding product with only 25% yield and 12% ee, which constituted the poorest result. Concerning the 2-aminonaphthalene partner, the nature of the substituent R⁵ was found to have a dramatic effect on the enantioselectivity. For example, products with electron-donating 3'-aryl groups (R⁵ = *p*-*t*-BuC₆H₄, *p*-Tol) were obtained with relatively lower enantioselectivities (72-74% ee vs 88-92% ee) in comparison with products bearing electron-withdrawing 3'-substituents (R⁵ = *p*-CF₃C₆H₄, 3,5-(CF₃)₂C₆H₃). On the other hand, the nature of the substituent R⁴ on the 2-aminonaphthalene had a negligible effect on the stereoselectivity of the process. In addition, both primary and secondary amines were compatible. The authors proposed that the chiral disulfonate iron complex could bind the two substrates and the oxidant, which allowed a high degree of chemo- and enantioselectivities to be achieved.



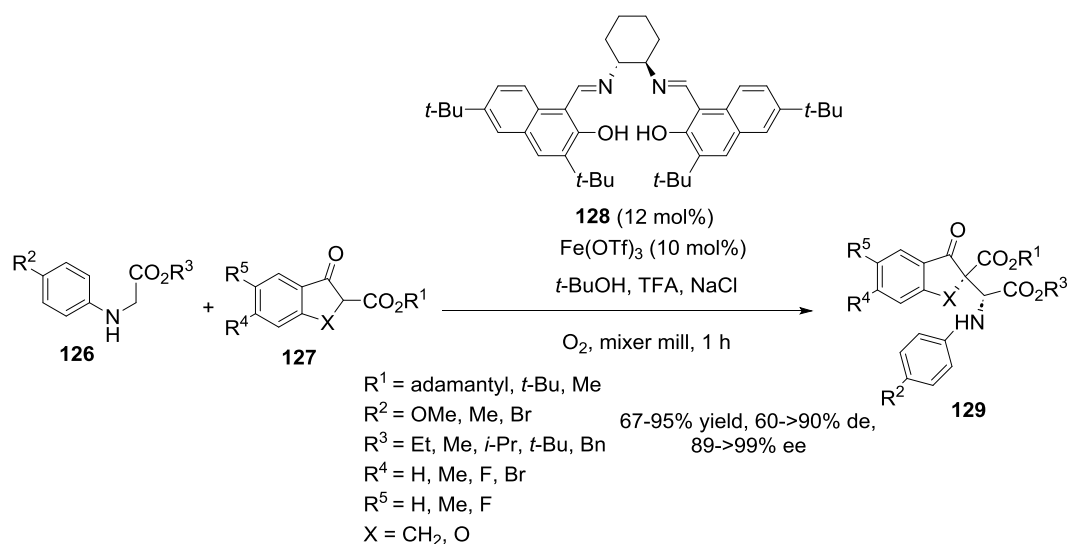
Scheme 34. Oxidative cross-coupling reaction of 2-naphthols with 2-aminonaphthalenes.

Heterobiaryl products with an axial chirality also constitute very important molecules, but their synthesis through direct oxidative couplings remain scarce. In 2023, Smith et al. described a very rare methodology of this type based on the use of a chiral iron catalyst in situ generated from 10 mol% of FeCl₃·6H₂O and 12 mol% of chiral Pybox ligand **122** (Scheme 35).⁴³ Thus, the direct coupling between 2-naphthols **123** and indoles **124** was achieved at room temperature within 16 hours in the presence of di-*tert*-butylperoxide as the oxidant in a 1:1 mixture of DCE and HFIP as the solvent to give the corresponding heterobiaryl products **125** with 13-97% yields and 20-96% ee. The process showed a remarkable chemoselectivity since it afforded exclusively the cross-coupled products without the competing homocoupling products. It was found that the presence of powerful electron-withdrawing substituents on the indole ring resulted in the obtention of decreased yields (R⁴ = CN: 13%, R⁴ = CF₃: 28%). Moreover, the size of the indole C-2 substituent (R²) was found crucial in determining the rotational barrier of the biaryl products. Indeed, changing a steric hindered substituent to a smaller group at this position, such as an *iso*-propyl, led to a significant reduction in the enantioselectivity (R² = *i*-Pr: 20% ee).



Scheme 35. Oxidative cross-coupling reaction of 2-naphthols with indoles.

The liquid-assisted grinding strategy is a useful technique derived from mechanochemistry in which tiny liquid additives, such as *t*-BuOH, participate in the catalytic cycle to endow high reactivity and enantioselectivity. Very recently, Yu et al. applied this protocol to enantioselective iron-catalysed asymmetric oxidative cross-coupling reaction between glycines **126** and β -ketoesters **127** (Scheme 36).⁴⁴ The C(sp³)-H/C(sp³)-H coupling was catalysed by a chiral complex in situ generated from Fe(OTf)₃ (10 mol%) and salen ligand **128** (12 mol%) in the presence of *t*-BuOH as an additive and NaCl. The media was milled with two stainless-steel balls under O₂, leading to a wide variety of chiral α -amino acid derivatives **129** with 67-95% yields, 60->90% de, and 89->99% ee. The authors demonstrated that the enantioselectivity of the process was dramatically improved in the ball-milling strategy in comparison with classical solution-stirred and neat-stirred approaches.

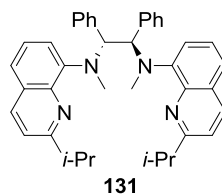
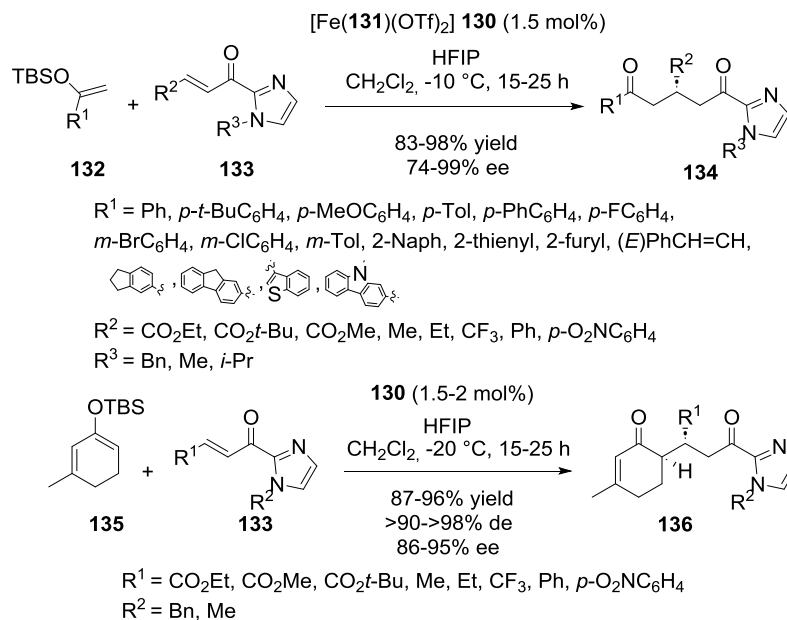


Scheme 36. Oxidative cross-coupling reaction of glycines with β -ketoesters.

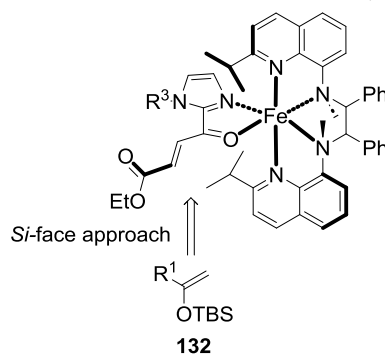
7. Michael-type reactions

In 2021, Che et al. developed enantioselective Michael additions of silyl enol ethers to α,β -unsaturated 2-acyl imidazoles to afford chiral 1,5-dicarbonyl products.⁴⁵ This was achieved by employing novel chiral iron catalyst **130** exhibiting a bulky tetradentate bis-(quinolyl)diamine chiral ligand **131** (Scheme 37). When 1.5 mol% of this preformed chiral complex was used at -10 °C in dichloromethane in the presence of HFIP as an additive, *t*-butyldimethylsilyl enol ethers **132** added to α,β -unsaturated 2-acyl imidazoles **133** to produce within 15-25 hours the corresponding chiral 1,5-dicarbonyl products **134** in 83-98% yields and 74-99% ee. The catalyst system was compatible with a wide range of (hetero)aromatic silyl enol ethers exhibiting either electron-donating or electron-withdrawing substituents on the phenyl ring, leading to products with uniformly excellent ee values (91-98% ee). However, a lower enantioselectivity (74% ee) was observed in the reaction of a styryl-substituted silyl enol ether (R¹ = (*E*)-PhCH=CH). The scope of the methodology was also extended to cyclic silyl enol ethers, such as cyclohexenone-derived one **135**, which could be added to a variety of α,β -unsaturated 2-acyl imidazoles **133** bearing ester, alkyl, and aryl β -substitutions, resulting in the formation of the desired chiral functionalised cyclohexenones **136** as almost single diastereomers (>90->98% de) in both very high yields (87-96%) and enantioselectivities (86-95% ee), as illustrated in Scheme 37. In this case, the Michael reaction was performed at -20 °C with 1.5-2 mol% of catalyst loading. A transition state depicted in Scheme 36 explains the stereoselectivity of the reaction between *t*-butyldimethylsilyl enol ethers **132** and α,β -unsaturated 2-acyl imidazoles **133** to give chiral products **134**. It shows that the imidazole is

activated through bidentate coordination to the iron centre. Since the *Re*-face of the C=C bond is sterically shielded by one of the isopropyl groups of the ligand, the silyl enol ether attacks from the less hindered *Si*-face of the double bond, leading to the (*S*)-configured product.



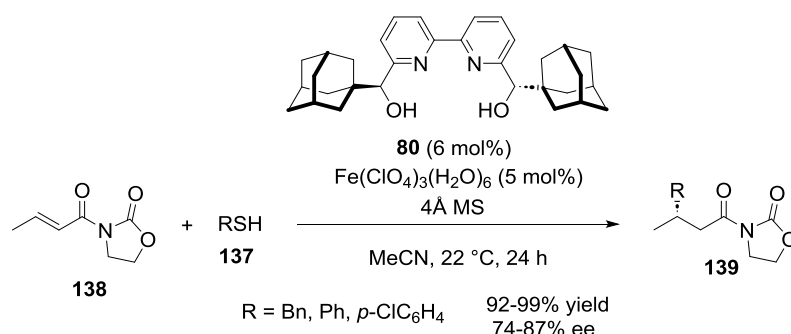
proposed transition state for the formation of **134** (with $\text{R}^2 = \text{CO}_2\text{Et}$):



Scheme 37. Michael additions of silyl enol ethers to α,β -unsaturated 2-acyl imidazoles.

In 2022, Ollevier et al. synthesised novel chiral 2,2'-bipyridine- α,α' -1-adamantyl-diol ligand **80** which was proven to be highly efficient promotor in enantioselective Michael additions of thiols **137** to α,β -unsaturated oxazolidin-2-ones **138** (Scheme 38).³⁰ The thio-Michael addition occurred at 22 °C in acetonitrile in the presence of 6 mol% of this bulky

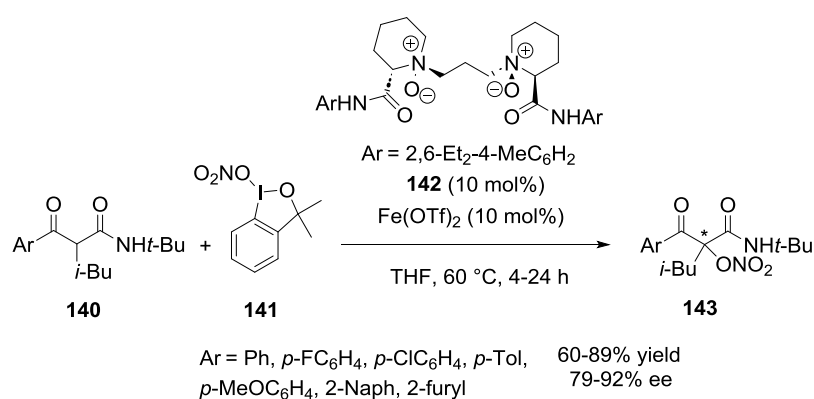
ligand associated with 5 mol% of $\text{Fe}(\text{ClO}_4)_3 \cdot 6\text{H}_2\text{O}$, leading within 24 hours to desired chiral thiols **139** with 92-99% yields and 74-87% ee.



Scheme 38. Michael addition of thiols to α,β -unsaturated oxazolidin-2-ones.

8. α -Functionalisations of carbonyl compounds

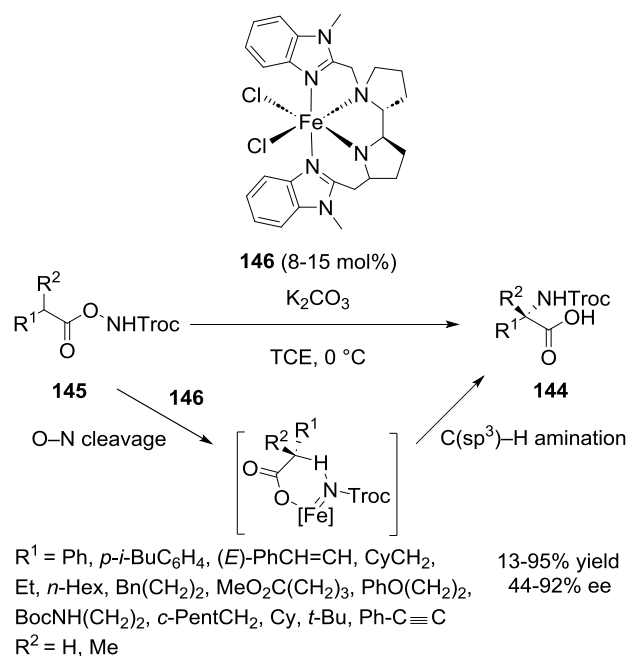
In 2022, Feng and Cao described enantioselective iron-catalysed nitroxylation of acyclic β -keto amides **140** with hypervalent iodine(III) reagents, such as nitratobenziodoxole **141** (Scheme 39).⁴⁶ The catalyst was in situ generated from 10 mol% of $\text{Fe}(\text{OTf})_2$ and the same quantity of chiral N,N' -dioxide ligand **142**. Performed at 60 °C in THF as the solvent, the reaction afforded within 4-24 hours chiral α -nitroxy- β -keto amides **143** in 60-89% yields and 79-92% ee. Aryl-substituted substrates exhibiting different groups on the phenyl ring reacted with high ee values (79-92% ee) as well as heteroaryl-substituted β -keto amides (Ar = 2-Naph, 2-furyl, 79-91% ee).



Scheme 39. Nitroxylation of acyclic β -keto amides with nitratobenziodoxole.

In the same year, Meggers and Chen disclosed an unprecedented catalytic synthesis of chiral α -amino acids **144** based on an enantioselective $\text{C}(\text{sp}^3)\text{-H}$ amination of azanyl esters

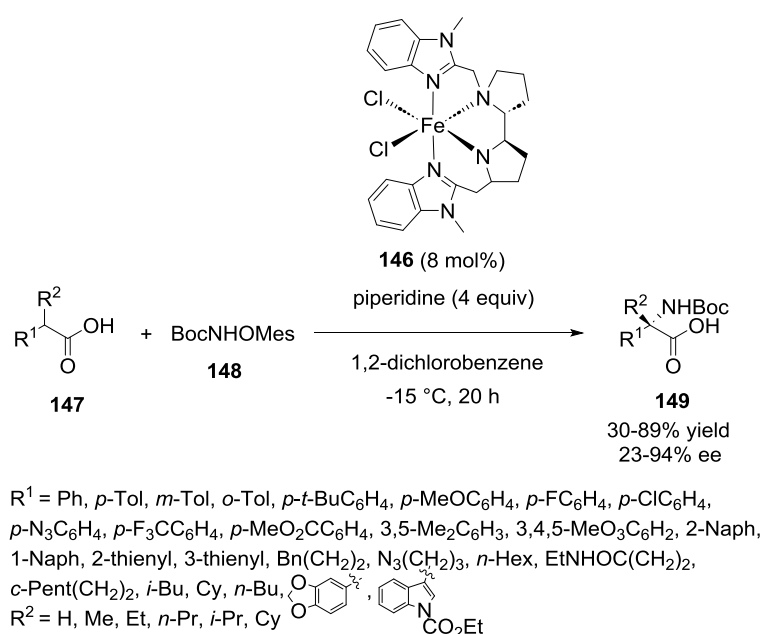
145 (Scheme 40).⁴⁷ This simple process was achieved at 0 °C by using chiral preformed iron catalyst **146** at 8-15 mol% of catalyst loading in TCE as the solvent. Under these mild conditions, readily available azanyl esters **145** underwent a stereocontrolled 1,3-nitrogen shift from one carboxylic acid oxygen to the α -carbon to give chiral α -amino acids **144** with 13-95% yields and 44-92% ee. This novel methodology offered a wide broad scope since α -amino acids bearing aryl, allyl, propargyl as well as alkyl (functionalised) side chains could be synthesised. As shown in Scheme 40, after the O–N bond cleavage in the azanyl ester followed by binding of both the two thus-formed fragments to the chiral catalyst, a cyclic transition state underwent stereocontrolled C(sp³)–H amination which produced the final α -amino acid.



Scheme 40. C(sp³)–H amination of azanyl esters.

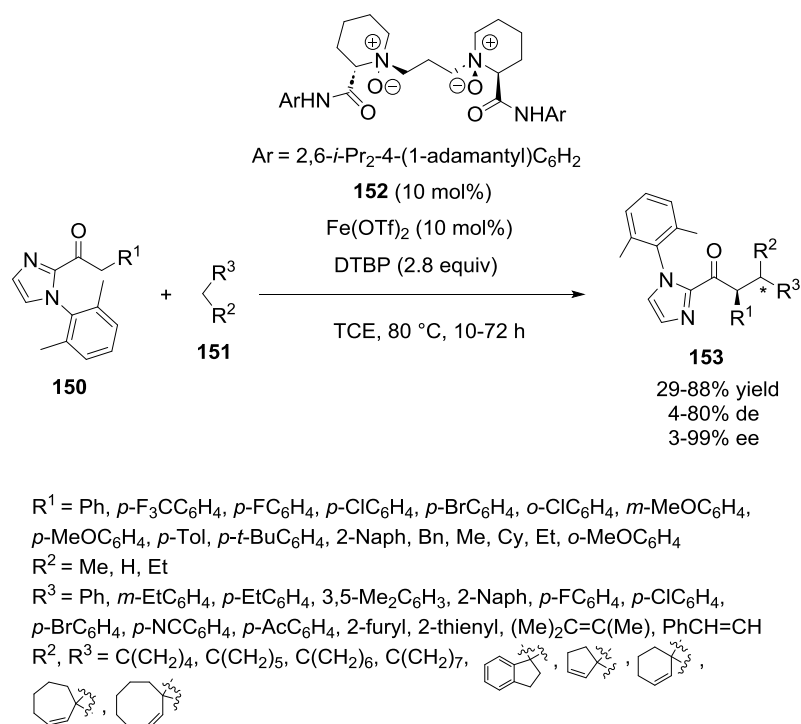
Later in 2023, the same group reported the direct C(sp³)–H amination of carboxylic acids **147** with *N*-Boc-protected carbamate **148** by using 8 mol% of the same catalyst system (Scheme 41).⁴⁸ In this case, the intermolecular reaction was carried out at -15 °C in 1,2-dichlorobenzene as the solvent in the presence of piperidine as a base. The directed α -C(sp³)–H nitrene insertion of a wide range of carboxylic acids led within 2 hours to the corresponding chiral α -amino acids **149** with 30-89% yields and 23-94% ee. The procedure was applicable to the synthesis of both α -monosubstituted and α,α -disubstituted amino acids, well tolerating the presence of either electron-donating or electron-withdrawing substituents on the phenyl ring

of the phenyl acetic acids. Interestingly, more challenging aliphatic carboxylic acids with non-activated C(sp³)-H bonds were also compatible, providing the desired products with enantioselectivities of up to 94% ee. Furthermore, the utility of this novel protocol was demonstrated by its application to diverse pharmaceutically relevant molecules, such as isoxepac, diclofenac, indomethacin, *tert*-butyldimethylsilyl-protected lithocholic acid, D-desthiobiotin, ibuprofen, ketoprofen, and naproxen, which all underwent stereocontrolled intermolecular amination with 37-88% yields and enantioselectivities of up to 91% e.e.



Scheme 41. Intermolecular direct C(sp³)-H amination of carboxylic acids.

In 2024, Feng and Liu reported the enantioselective α -alkylation of acyclic 2-acylimidazoles **150** through dehydrogenative radical cross-coupling with unactivated hydrocarbons **151** (Scheme 42).⁴⁹ The reaction was catalysed at 80 °C by 10 mol% of Fe(OTf)₂ combined with 10 mol% of chiral *N,N'*-dioxide ligand **152** in TCE as the solvent in the presence of di-*tert*-butyl peroxide (DTBP) as an oxidant, thus leading within 10-72h to a wide range of chiral acyclic carbonyl derivatives **153** with 29-88% yields, 4-80% de, and 3-99% ee. This simple oxidative cross-coupling methodology enabled the activation of inert C(sp³)-H bonds into a diversity of benzylic, allylic hydrocarbons, as well as nonactivated alkanes, with enantioselectivities of up to 99% ee.

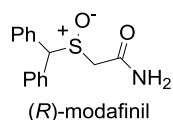
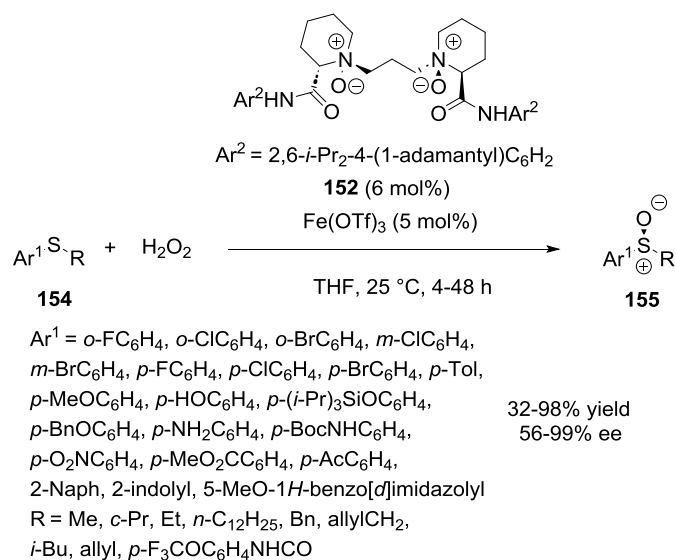


Scheme 42. α -Alkylation of acyclic 2-acylimidazoles with hydrocarbons.

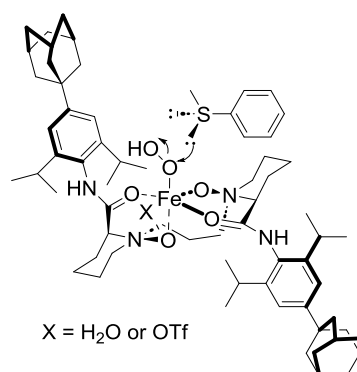
9. Sulfoxidations

The importance of chiral sulfoxides is related to their wide application in asymmetric synthesis as chiral ligands and catalysts,⁵⁰ as well as reagents and auxiliaries,⁵¹ but also to their presence among numerous drugs.⁵² Consequently, the synthesis of these compounds has attracted considerable attention.⁵³ Among the methodologies for their preparation, an enantioselective iron-catalysed sulfoxidation of alkyl aryl sulfides **154** was described by Feng and Dong, in 2020 (Scheme 43).⁵⁴ The procedure was based on the use of environmentally benign aqueous H₂O₂ as the oxidant. It involved an iron catalyst in situ generated from 6 mol% of chiral *N,N'*-dioxide ligand **152** and 5 mol% of Fe(OTf)₃ as the precatalyst in THF as the solvent. The asymmetric sulfoxidation of sulfides **154** performed at 25 °C led within 4-48 hours to the corresponding chiral sulfoxides **155** in 32-98% yields and 56-99% ee. In general, the reaction of aryl methyl sulfides (R = Me) provided better ee values (72-99% ee) than that of other aryl alkyl sulfides (56-94% ee with R \neq Me). The utility of this methodology was demonstrated in a synthesis of the drug (*R*)-modafinil. The stereoselectivity of the reaction can be explained by the transition state depicted in Scheme 43 in which the tetradentate chiral ligand and OOH⁻ coordinate with Fe(III) through an octahedral fashion. The steric repulsion between the aryl group in the sulfide and the neighboring 2,6-diisopropyl-4-(1-

adamantyl)phenyl group of the ligand discriminates the heterotopic lone pairs, which involves the privileged formation of the (*S*)-configured sulfoxide product.



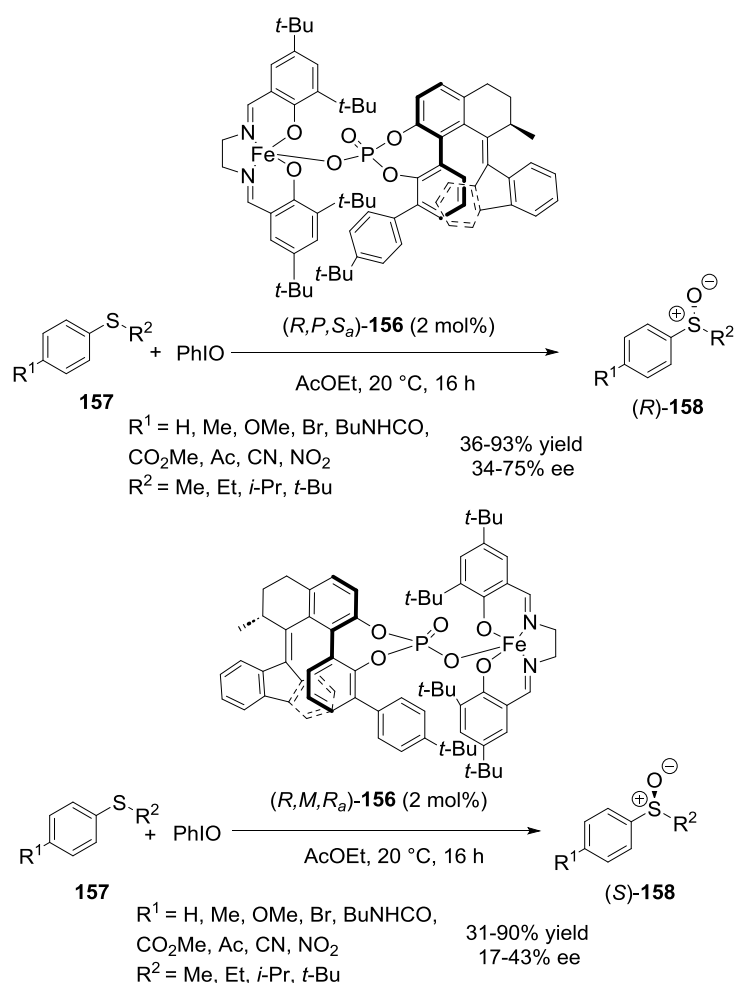
proposed transition state (with $\text{Ar}^1 = \text{Ph}, \text{R} = \text{Me}$):



Scheme 43. Sulfoxidation with hydrogen peroxide.

In 2023, Feringa, Nolte and Elemans described the synthesis and characterisation through X-ray analysis of novel photoswitchable iron(III) salen phosphate complex (*R,P,S_a*)-**156**.⁵⁵ The latter was further investigated to promote the enantioselective oxidation of alkyl aryl sulfides **157** into chiral sulfoxides (*R*)-**158** by using iodosylbenzene as the oxidant (Scheme 44). The reaction performed with 2 mol% of catalyst (*R,P,S_a*)-**156** in ethyl acetate as the solvent resulted within 16 hours in the formation at 20 °C of a range of (*R*)-configured sulfoxides **158** with 36-93% yields and 34-75% ee. The lowest ee values were observed in the reaction of electron-rich sulfides ($\text{R}^1 = \text{OMe}$: 34% ee) while electron-deficient sulfides led to

the desired products with higher enantioselectivities ($R^1 = \text{NO}_2$: 75% ee). The authors showed that using pseudoenantiomeric complex (R,M,R_a) -**156** prepared through photochemical isomerisation of (R,P,S_a) -**156** allowed under the same reaction conditions to synthesise chiral enantiomeric alkyl aryl sulfoxides (S) -**158** with 31-90% yields and 17-43% ee (Scheme 44). Therefore, the enantiodivergent oxidation of prochiral aryl alkyl sulfides to chiral aryl alkyl sulfoxides was achieved with the stable (S) -axial isomer of the catalyst producing the (R) -configured sulfoxides in up to 75% ee, whereas the photoisomerised metastable (R) -axial isomer of the catalyst favored the formation of the (S) -configured sulfoxides in up to 43% ee.

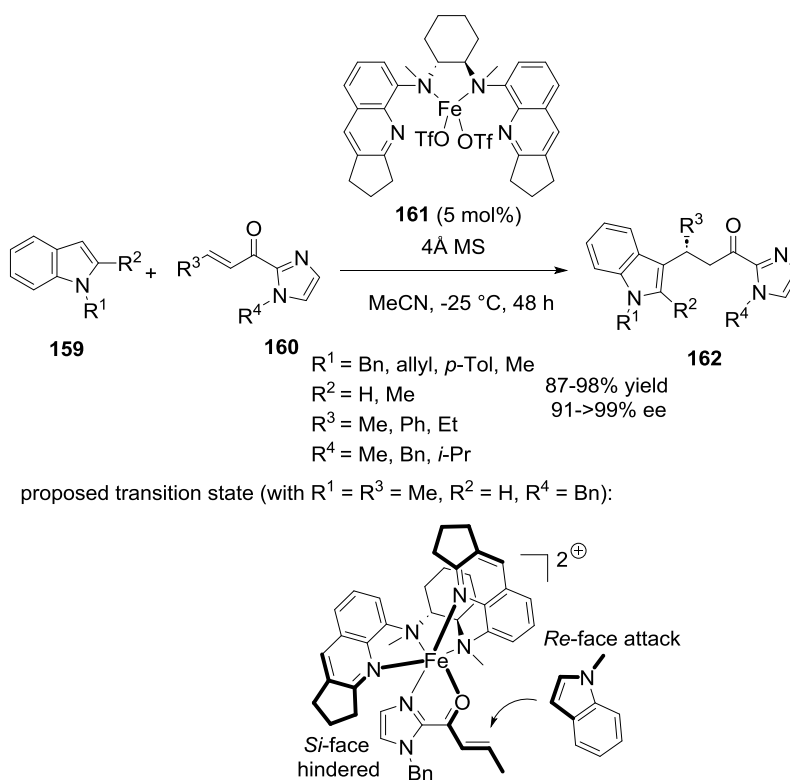


Scheme 44. Sulfoxidations with iodosylbenzene.

10. Alkylations of indoles

In 2020, Che et al. developed an enantioselective C3 alkylation of 2-substituted *N*-protected indoles **159** with α,β -unsaturated 2-acyl imidazoles **160** catalysed by preformed chiral iron complex **161** derived from a tetradentate bis(quinolyl)diamine N4 ligand.⁵⁶

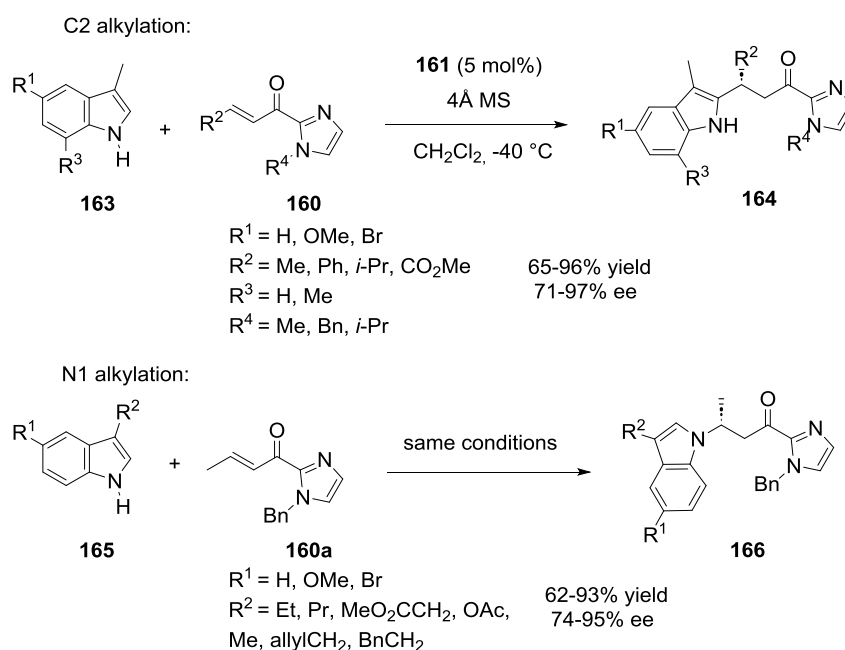
Performed in acetonitrile at $-25\text{ }^{\circ}\text{C}$ in the presence of 5 mol% of this catalyst, the reaction regioselectively afforded within 48 hours a variety of chiral indoles **162** with 87-98% yields and 91->99% ee (Scheme 45). Noteworthy, no C2 alkylation product was observed. Neither β - nor N-substitution of α,β -unsaturated 2-acyl imidazoles was found to have a significant impact on the enantioselectivity of the reaction. Moreover, variously 2- and N-substituted indoles were compatible. The thus-formed products could be converted into a variety of chiral indole derivatives with potential synthetic and biological values. The authors proposed the transition state depicted in Scheme 45 in which the imidazole coordinated to the catalyst through its carbonyl oxygen and imidazolyl nitrogen atoms. Then, the indole attacked from the *Re*-face since the *Si*-face was sterically hindered by the chiral environment around the iron centre.



Scheme 45. C3 alkylation of 2-substituted *N*-protected indoles with α,β -unsaturated 2-acyl imidazoles.

The same catalyst was also applied to achieve enantio- and regioselective C2 alkylation of unprotected 3-methylindoles **163** with α,β -unsaturated 2-acyl imidazoles **160**. The reaction was performed in this case at $-40\text{ }^{\circ}\text{C}$ in dichloromethane with the same catalyst loading.⁵⁶ The

corresponding chiral C2 alkylated indoles **164** were obtained regioselectively with 65-96% yields and 71-97% ee (Scheme 46). It was found that the regioselectivity of the reaction was changed from C2 to N1 alkylation in the reaction of other 3-substituted indoles **165** with α,β -unsaturated 2-acyl imidazole **160a** according to the electronic and steric nature of the substituent on the indoles (R^2 in **165**), as detailed in Scheme 43. Moreover, the electronic nature of the substituent exhibited on the α,β -unsaturated 2-acyl imidazoles (R^2 in **160**) was also important on determining the C2 or N1 regioselectivity of the reaction. A range of N1 alkylated chiral products **166** could be synthesised in 65-93% yields and 74-95% ee. This methodology was applied to the synthesis of potent intermediates in medicinal chemistry.

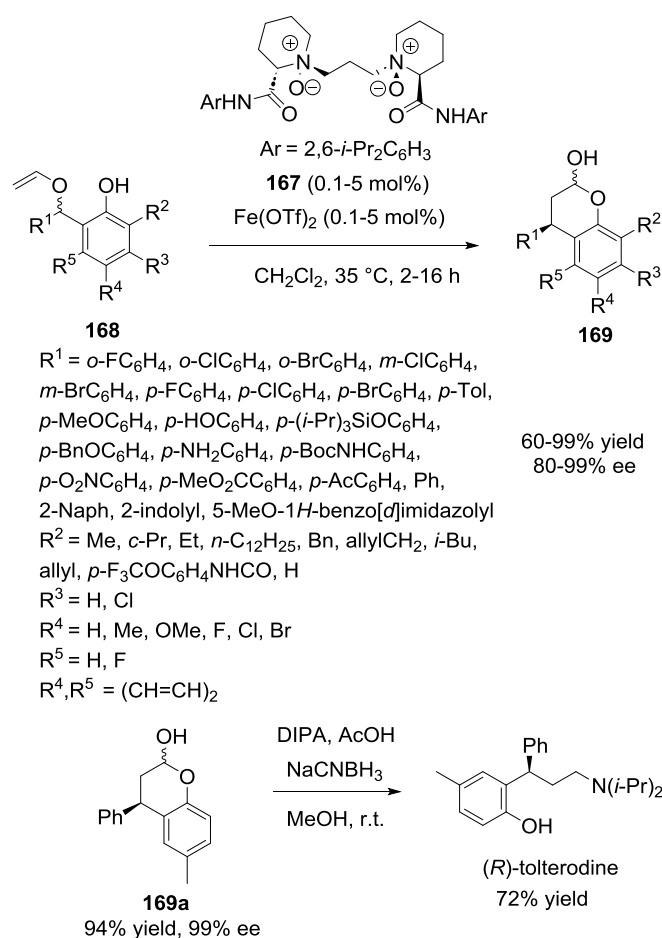


Scheme 46. C2 and N1 alkylations of 3-substituted indoles with α,β -unsaturated 2-acyl imidazoles.

11. Rearrangement reactions

Substituted chromanols and chromanones represent key structural motifs in many drugs and natural products. Consequently, efficient enantioselective methodologies for their synthesis are challenging. In this context, Feng and Liu employed in 2020 chiral N,N' -dioxide ligand **167** combined with an iron precatalyst to promote highly enantioselective [1,3] rearrangement of 2-vinylloxymethylphenols **168** (Scheme 47).⁵⁷ Indeed, a range of variously substituted 2-vinylloxymethylphenols **168** rearranged at 35 °C within 2-16 hours in the presence of only 0.1-5 mol% of iron catalyst derived from $\text{Fe}(\text{OTf})_2$ and ligand **167** in

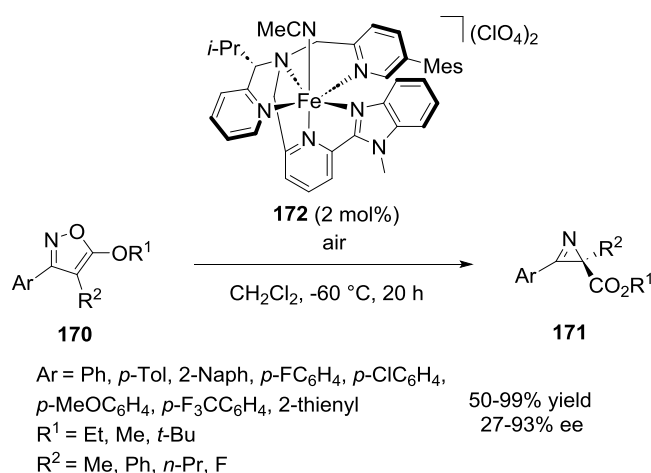
dichloromethane as the solvent to afford the corresponding chiral chromanols **169** with 60-99% yields and 80-99% ee. Uniformly excellent ee values (96-99% ee) were obtained for aryl-substituted substrates with either electron-donating or electron-withdrawing substituents at *ortho*-, *meta*- or *para*-positions of the phenyl ring ($R^1 = \text{aryl}$). Furthermore, comparable very high enantioselectivities were achieved in the reaction of a series of alkyl-substituted 2-vinyloxymethylphenols ($R^1 = \text{alkyl}$). The presence of electron-withdrawing or electron-donating groups at the phenol (R^2 - R^5) unit had no impact on the enantioselectivity of the process (80-99% ee). The utility of this methodology was applied to develop a total synthesis of the anticholinergic drug (*R*)-tolterodine (Scheme 47).



Scheme 47. [1,3]-Rearrangement of alkyl vinyl ethers and synthesis of (*R*)-tolterodine.

In 2021, another type of asymmetric iron-catalysed rearrangement was described by Meggers et al.⁵⁸ It involved the ring contraction of isoxazoles **170** into the corresponding chiral 2H-azirines **171** (Scheme 48). To this aim, the authors introduced novel preformed chiral iron catalyst **172** based on a chiral pentadentate ligand coordinating to a central iron(II)

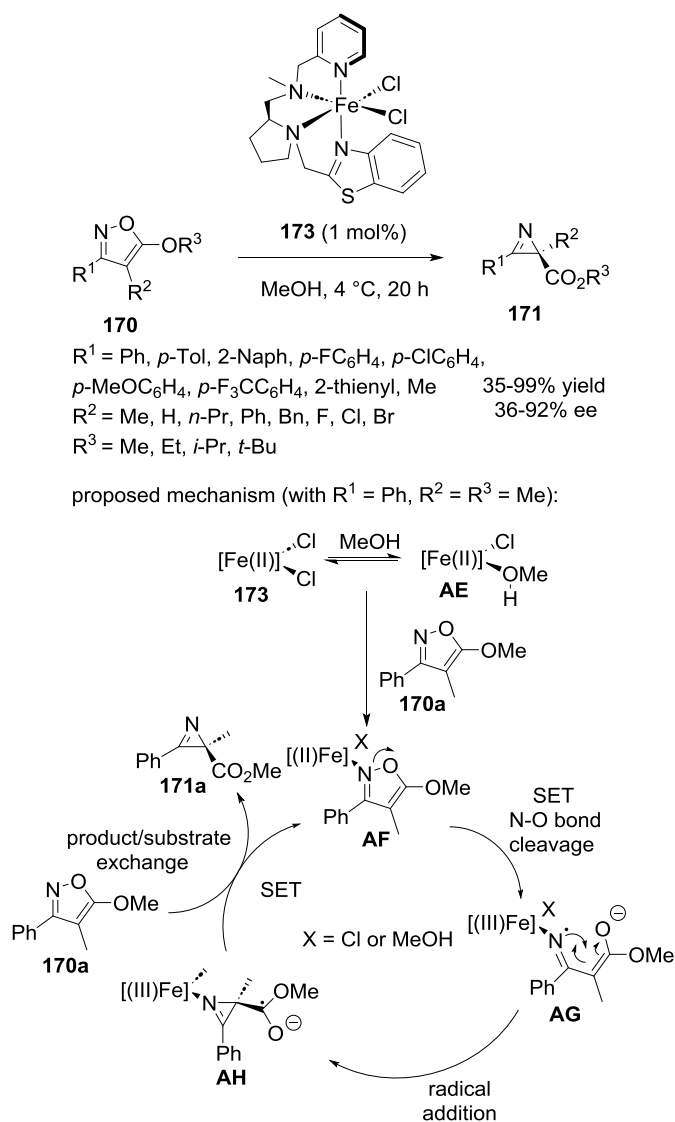
through a tripodal fashion. When 2 mol% of this complex was applied in dichloromethane at -60 °C to promote this reaction, it resulted within 20 hours in the formation of a range of chiral 2H-azirines **172** in 50-99% yields and 27-93% ee. The influence of the nature of the alkoxy moiety (R^1) on the substrate was found important since all methoxy and ethoxy esters reacted smoothly to give the desired 2H-azirines in uniformly high enantioselectivities (82-93% ee), whereas the reaction of a sterically hindered *tert*-butoxy ester ($R^1 = t\text{-Bu}$) provided a much lower ee value (27% ee). This could be rationalised by the bulky *tert*-butyl group interfering with the coordination of the substrate to the catalyst. Moreover, different (hetero)aryl substituents (Ar) were compatible, providing high ee values whatever the electronic nature of the substituents present on the phenyl ring. The influence of the substituent on the 4-position of the isoxazole (R^2) was also investigated, showing that either methyl- or phenyl-substituted substrates afforded good results (74-93% ee) while lower ee values (68-73% ee) were obtained in the reaction of isoxazoles bearing a propyl group or a fluorine atom in this position.



Scheme 48. Rearrangement of isoxazoles into 2H-azirines with catalyst **162**.

Later in 2023, the same group reinvestigated these reactions by using novel non- C_2 -symmetric chiral iron(II) catalyst **173** based on a chiral tetradentate N₄-ligand (Scheme 49).⁵⁹ In this case, a lower catalyst loading (1 mol%) was capable of promoting the ring contraction reaction which was performed at higher temperature (4 °C vs -60 °C) in methanol as the solvent. Under these novel conditions, a range of chiral 2H-azirines **171** were produced within 20 hours with 35-99% yields and 36-92% ee. The lowest ee value (36% ee) was observed in the reaction of an alkyl-substituted ($R^1 = \text{Me}$) isoxazole. The authors proposed the mechanism

described in Scheme 49, beginning with the coordination of the isoxazole to the supposed active catalyst species **AE** or eventually to catalyst **173** which generated iron intermediate **AF**. Then, a single electron transfer induced the cleavage of the N–O bond to give radical anion intermediate **AG**. Intramolecular radical addition of the latter species furnished radical anion **AH** which reduced the iron back to Fe(II). Finally, product/substrate exchange closed the catalytic cycle.

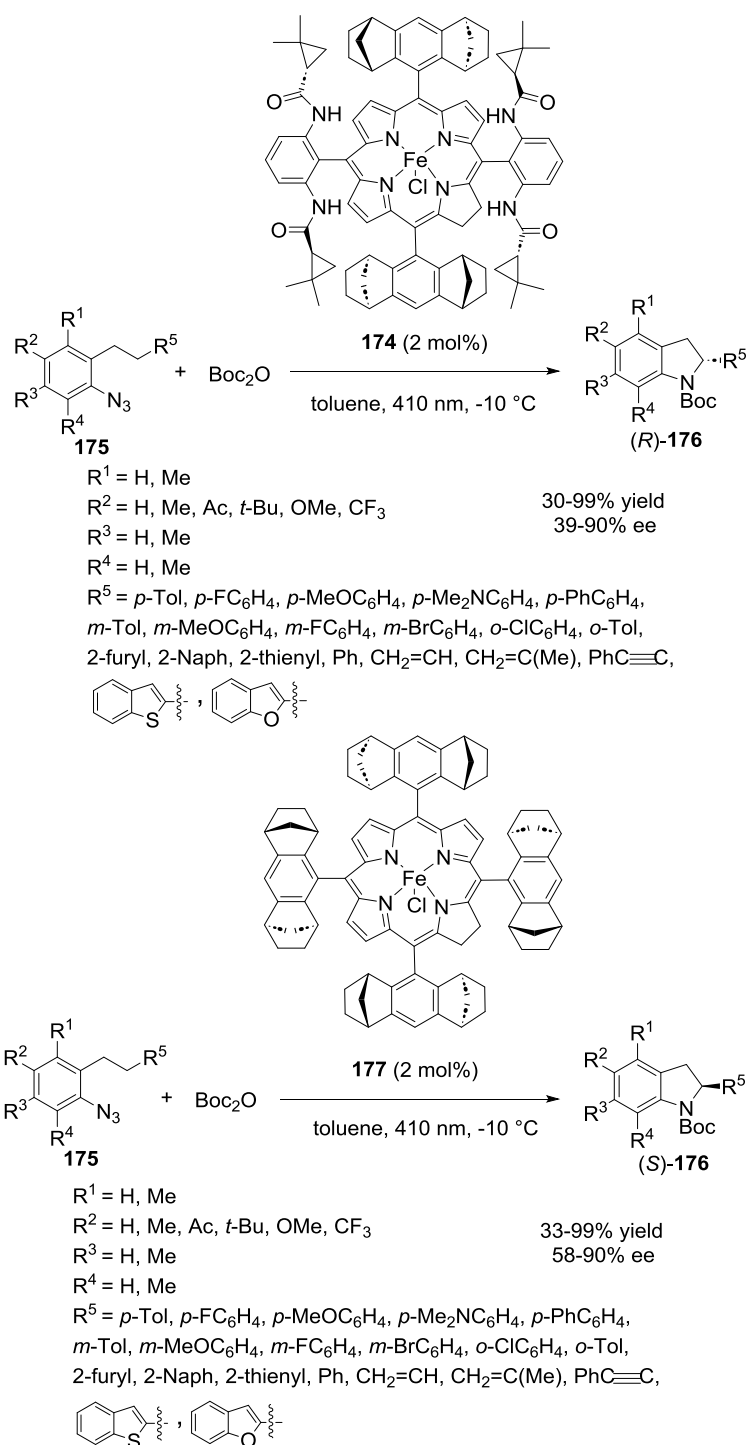


Scheme 49. Rearrangement of isoxazoles into 2H-azirines with catalyst **163**.

12. Intramolecular aminations

Examples of iron-catalysed asymmetric amination of C-(sp³)-H bonds remain rare. In 2023, Che, Liu and Dang described novel chiral iron porphyrin complexes that were

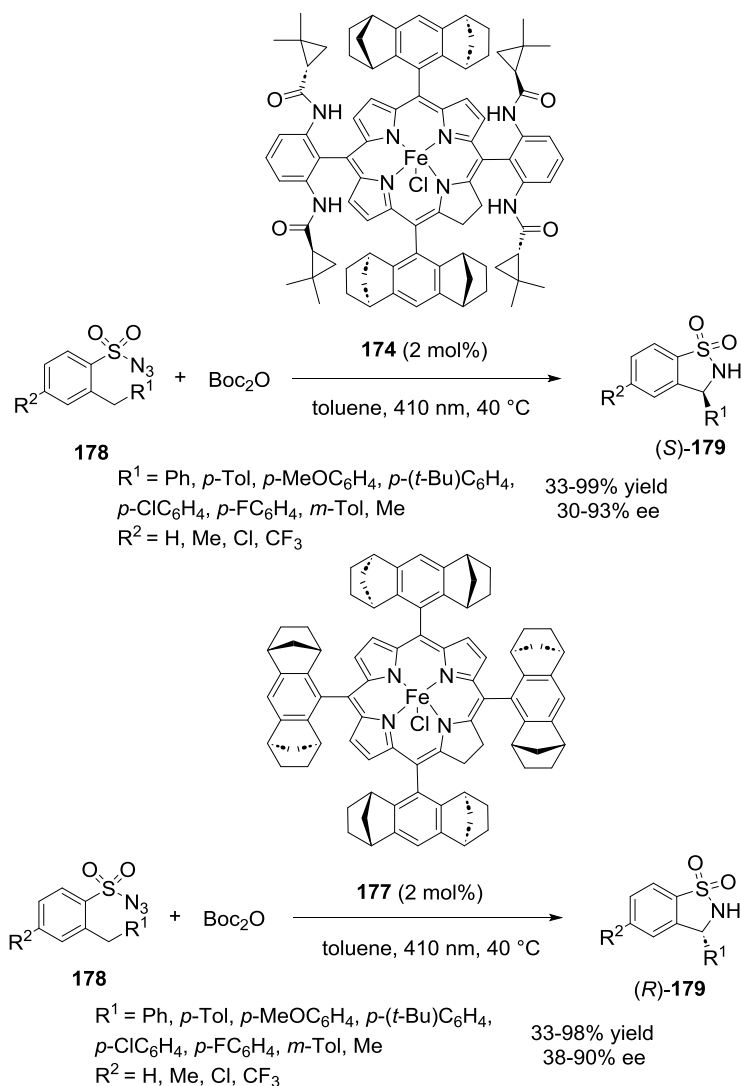
demonstrated to be highly efficient promoters of enantioselective C(sp³)-H aminations of aryl and arylsulfonyl azides.⁶⁰ By using 2 mol% of chiral iron catalyst **174** in toluene at -10 °C under visible light irradiation, a range of aryl azides **175** reacted with Boc₂O to afford the corresponding (*R*)-configured indolines **176** with 30-99% yields and 39-90% ee (Scheme 50). The authors found that when the same reaction was catalysed by chiral porphyrin complex **177** under the same conditions, it led to the enantiomeric (*S*)-configured indolines **176** with comparable yields (33-99%) and ee values (58-90% ee).



Scheme 50. Aminations of $\text{C}(\text{sp}^3)\text{-H}$ bonds of aryl azides.

The same chiral catalysts were also applied to promote the asymmetric intramolecular $\text{C}(\text{sp}^3)\text{-H}$ amination of arylsulfonyl azides **178** (Scheme 51). When the reaction was performed at 40°C in the presence of 2 mol% of catalyst **174**, the corresponding (*S*)-configured benzofused cyclic sulfonamides **179** were generated with 33-99% yields and en30-93% ee. On the other hand, enantiomeric (*R*)-configured sultams **179** were produced with

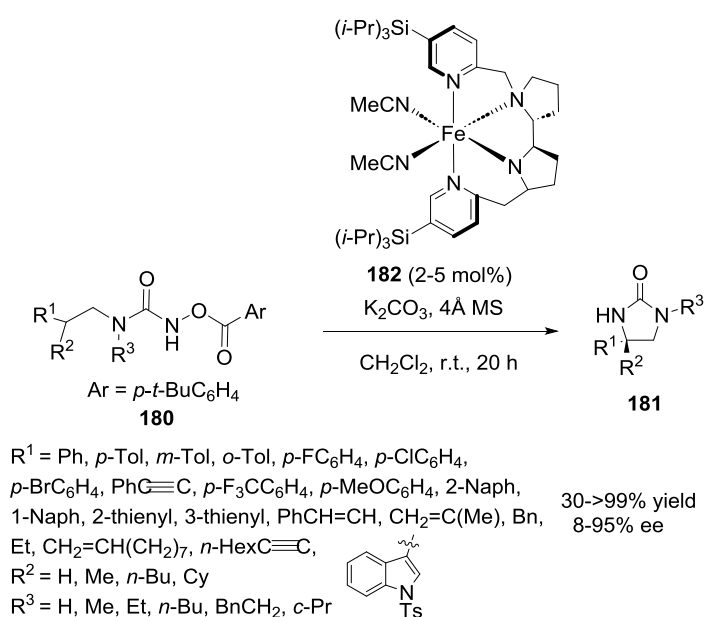
comparable results (33-98% yield, 38-90% ee) by employing 2 mol% of chiral porphyrin catalyst **177**.



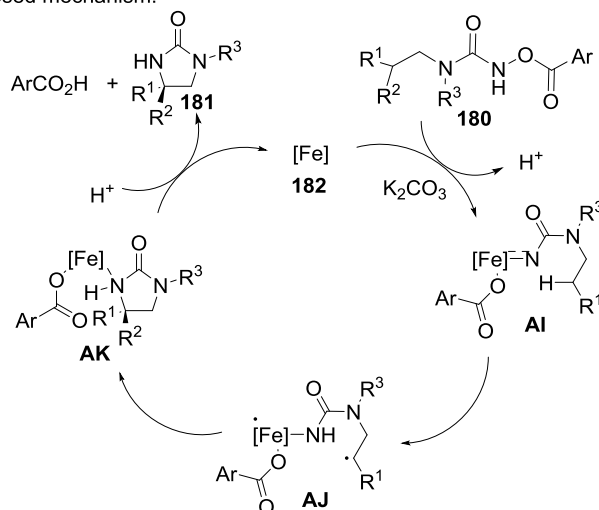
Scheme 51. Aminations of $\text{C}(\text{sp}^3)\text{-H}$ bonds of arylsulfonyl azides.

In 2023, Meggers et al. reported for the first time enantioselective iron-catalysed ring-closing aminations of *N*-aroyloxyureas **180**, allowing the synthesis of chiral 2-imidazolidinones **181**, which represent key building blocks in medicinal chemistry (Scheme 52).⁶¹ These intramolecular ring-closing $\text{C}(\text{sp}^3)\text{-H}$ aminations smoothly occurred at room temperature in dichloromethane in the presence of 2-5 mol% of chiral iron catalyst **182** derived from a tetradentate bis(pyridylmethyl)diamine ligand. A wide range of 4-monosubstituted 2-imidazolidinones ($\text{R}^2 = \text{H}$) could be synthesised within 20 hours under these mild conditions with 30->99% yields and 30-95% ee. Furthermore, the catalyst system

was also compatible with the preparation of 4,4-disubstituted 2-imidazolidinones ($R^2 \neq H$) with 30->99% yields and 8-93% ee. A possible radical mechanism is detailed in Scheme 52, in which the iron catalyst promoted the N—O cleavage of the *N*-aroyloxyurea induced by K_2CO_3 , which generated iron nitrene species **AI**. Then, the latter in its triplet state underwent a 1,5-hydrogen atom transfer to give diradical intermediate **AJ**. Subsequently, the C—N bond formation produced iron intermediate **AK**, which delivered the final product along with regenerated active catalyst.



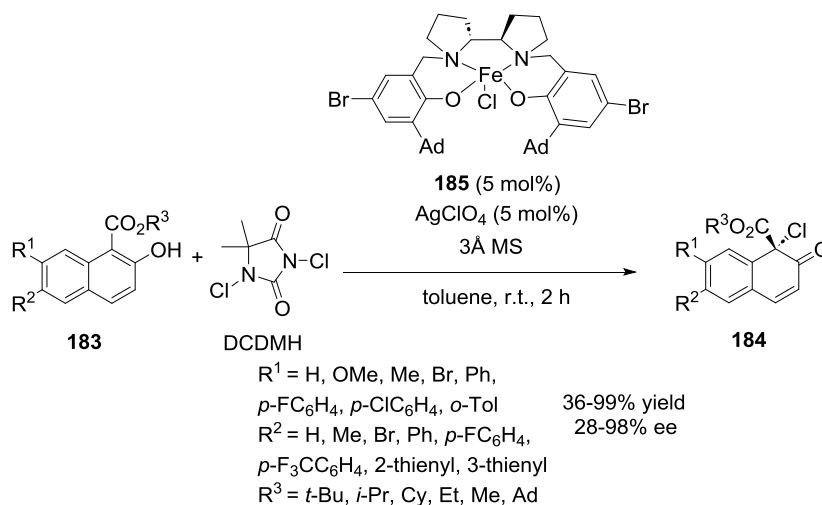
proposed mechanism:



Scheme 52. Amination of *N*-aroyloxyureas.

13. Miscellaneous reactions

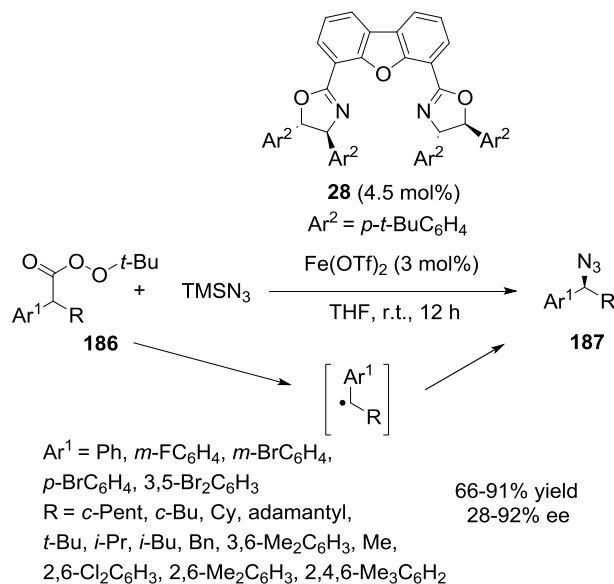
In 2021, Che and Xu reported an enantioselective dearomative chlorination of 2-hydroxy-1-naphthoates **183** to afford the corresponding chiral chlorinated products **184**.⁶² This practical methodology involved the use of 5 mol% of chiral preformed bipyrrolidine salan iron catalyst **185** in toluene at room temperature and 1,3-dichloro-5,5-dimethylhydantoin (DCDMH) as the chlorination agent. Performed in the presence of 5 mol% of AgClO₄ as an additive, the asymmetric α -halogenation of various 2-hydroxy-1-naphthoate derivatives **133** bearing different substituents allowed the desired chiral naphthalenones **184** exhibiting a quaternary chlorinated stereocenter to be achieved within 2 hours in 36-99% yields and 28-98% ee (Scheme 53). The authors found that the size of the ester group (R³) played an important role in the enantioselectivity of the reaction. Indeed, a sterically hindered group, such as a *tert*-butyl ester, led to higher enantioselectivities (85-98% ee) than smaller ones, such as methyl, ethyl, cyclohexyl, and *i*-propyl groups (40-71% ee). The presence of different electron-donating substituents on the naphthalene ring was well tolerated while a substrate substituted by an electron-withdrawing bromide substituent (R¹ = Br) underwent the reaction to afford the corresponding chlorinated product with a lower ee value (52% ee).



Scheme 53. Dearomative chlorination of 2-hydroxy-1-naphthoates.

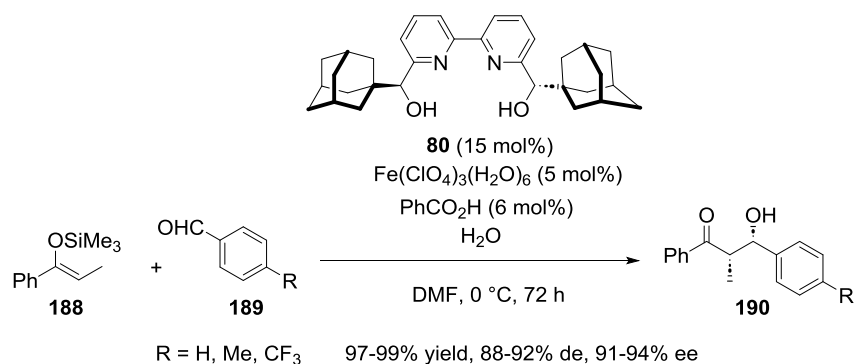
The same year, Bao and Li disclosed the first example of enantioselective iron-catalysed radical azidation of benzylic peresters with TMSN₃ as the azido source.⁶³ The decarboxylative azidation reaction was promoted by a chiral catalyst in situ generated from 3 mol% of Fe(OTf)₂ and 4.5 mol% of chiral bisoxazoline ligand **28**. The reaction of a range of benzylic peresters **186** with TMSN₃ led within 12 hours at room temperature in THF to the corresponding chiral azides **187** with 66-91% yields and 28-92% ee (Scheme 54). A broad

substrate scope was compatible with generally high ee values achieved in the reaction of sterically hindered substrates. For example, less sterically hindered methyl-substituted substrate (R = Me) provided the corresponding product with only 28% ee.



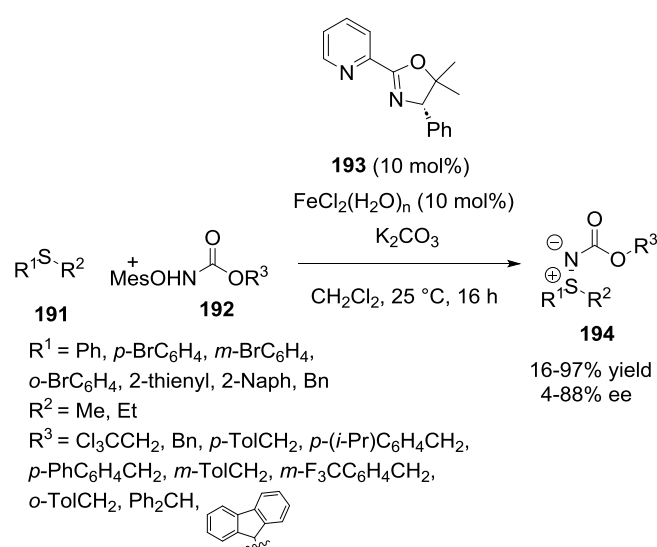
Scheme 54. Decarboxylative azidation of benzylic peresters with TMSN₃.

In 2022, Ollevier et al. synthesised novel chiral 2,2'-bipyridine- α,α' -1-adamantyl-diol ligand **80** which was investigated to promote enantioselective Mukaiyama aldol of (*Z*)-silyl enol ether **188** with benzaldehydes **189**.³⁰ This ligand was employed at 15 mol% of catalyst loading with 5 mol% of Fe(ClO₄)₃·6H₂O in DMF as the solvent. The reaction led within 72 hours at 0 °C to chiral *syn*-aldol products **190** with 97-99% yields with both excellent diastereo- (88-92% de) and enantioselectivities (91-94% ee), as shown in Scheme 55.



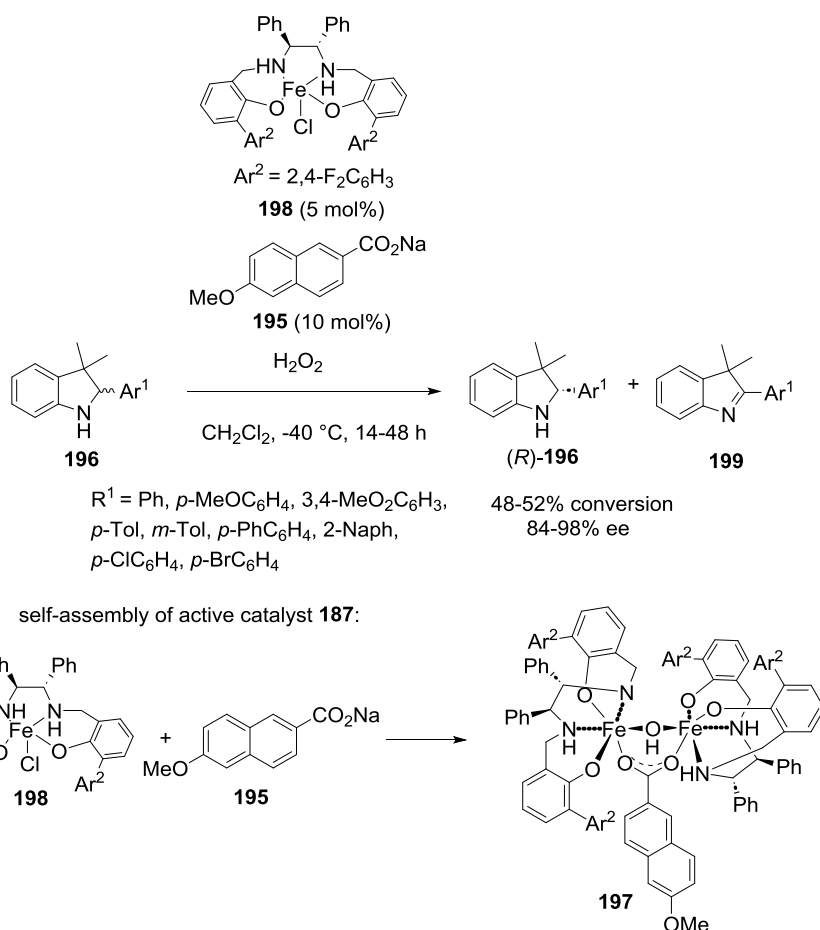
Scheme 55. Mukaiyama aldol of a (*Z*)-silyl enol ether with benzaldehydes.

The same year, Lebel and Lai developed the first iron-catalysed enantioselective amination of thioethers **191** with *N*-mesyloxycarbamates **192** as nitrene precursors (Scheme 56).⁶⁴ The authors selected chiral pyridine oxazoline **193** as optimal ligand employed at 10 mol% of catalyst loading in combination with 10 mol% of FeCl₂ as the precatalyst. The reaction was performed at 25 °C in dichloromethane in the presence of K₂CO₃ as a base to give within 16 hours chiral sulfilimines **194** with 16-97% yields and 4-88% ee. Actually, the ee values were generally modest (≤44% ee) excepted in the reaction of an *ortho*-substituted sulfilimine (R¹ = *o*-BrC₆H₄, R² = Ph, R³ = CHPh₂) which led to the desired product with 88% ee albeit combined with a low yield (17%).



Scheme 56. Amination of thioethers with *N*-mesyloxycarbamates.

Novel chiral diiron(III) dimer complexes based on salan ligands were designed in 2022 by Liu et al. to be used for the first time as promoters in dehydrogenative kinetic resolution of indolines **196** using environmentally benign hydrogen peroxide as the oxidant (Scheme 57).⁶⁵ The active dinuclear complex **197** bearing sterically encumbered salan ligands and a 2-naphthoate bridge was in situ generated by self-assembly of iron complex **198** with sodium aryl carboxylate **195**. This diiron complex was revealed to be an efficient promoter in the asymmetric dehydrogenation of indolines **196** performed at -40 °C in dichloromethane, resulting within 14-48 hours in the recovering of (*R*)-configured indolines **196** with good conversions (48-52%) and homogeneously high ee values (84-98% ee) along with imines **199**.



Scheme 57. Dehydrogenative kinetic resolution of indolines.

14. Conclusions

This review demonstrates that as a cheaper and less toxic metal in comparison to traditional metals, iron has gained a significant importance in green catalysis, offering an alternative to replace toxic metals in the near future. Indeed, chiral iron catalysts are more and more applied to promote an increasing diversity of enantioselective transformations. This review updates this field since the beginning of 2020, demonstrating that, whilst still in its infancy, asymmetric iron catalysis is growing rapidly. It illustrates the power of these green catalysts to promote all types of highly enantioselective transformations, such as domino reactions, reductions of ketones and imines, cycloadditions, additions to alkenes, coupling reactions, Michael-type reactions, α -functionalisations of carbonyl compounds, sulfoxidations, alkylations of indoles, rearrangement reactions, intramolecular aminations, and miscellaneous reactions, providing an enormous potential for greener synthesis. Further developments in this field are awaited in the near future with the involvement of other types of chiral ligands and their application to other transformations to definitively establish iron as

a potential pillar in the discipline of green catalysis with reduced environmental impacts coupled with the potentially lower toxicity showing promise toward applications in both medicinal and pharmacological fields.

Acknowledgements

This work was supported by the National Centre for Scientific Research: CNRS.

References and notes

- (a) Noyori, R. *Asymmetric Catalysts in Organic Synthesis*; Wiley-VCH: New-York; **1994**; (b) Nogradi, M. *Stereoselective Synthesis*; Wiley-VCH: Weinheim; **1995**; (c) Beller, M.; Bolm, C. *Transition Metals for Organic Synthesis*; Wiley-VCH: Weinheim, **1998**, Vols I and II; (d) E.N. Jacobsen, A. Pfaltz, H. Yamamoto, *Comprehensive Asymmetric Catalysis*, Springer: New York, 1999; (e) Ojima, I. *Catalytic Asymmetric Synthesis*; second ed., Wiley-VCH: New-York, **2000**; (f) Poli, G.; Giambastiani, G.; Heumann, A. *Tetrahedron* **2020**, *56*, 5959–5989; (g) Negishi, E. *Handbook of Organopalladium Chemistry for Organic Synthesis*; John Wiley & Sons: Hoboken NJ, **2002**; (h) de Meijere, A.; von Zezschwitz, P.; Nüske, H.; Stulgies, B. *J. Organomet. Chem.* **2002**, *653*, 129–140; (i) Beller, M.; Bolm, C. *Metals for Organic Synthesis*; second ed., Wiley-VCH: Weinheim, **2004**; (j) Tietze, L. F.; Hiriyakkanavar, I.; Bell, H. P. *Chem. Rev.* **2004**, *104*, 3453–3516; (k) Ramon, D. J.; Yus, M. *Chem. Rev.* **2006**, *106*, 2126–2208; (l) Pellissier, H. *Coord. Chem. Rev.* **2015**, *284*, 93–110; (m) Bryliakov, K. P. *Chem. Rev.* **2017**, *117*, 11406–11459; (n) Pellissier, H. *Synthesis* **2021**, *53*, 1379–1395; (o) Pellissier, H. *Coord. Chem. Rev.* **2021**, *439*, 213926; (p) Pellissier, H. *Coord. Chem. Rev.* **2022**, *463*, 214537.
- (a) Fürstner, A. *ACS Cent. Sci.* **2016**, *2*, 778–789; (b) Rana, S.; Prasad Biswas, J.; Paul, S.; Paik, A.; Maiti, D. *Chem. Soc. Rev.* **2021**, *50*, 243–472.
- Casnati, A.; Lanzi, M.; Cera, G. *Molecules* **2020**, *25*, 3889–3928.
- (a) Pellissier, H. *Coord. Chem. Rev.*, **2019**, *386*, 1–31; (b) Ollevier, T. *Catal. Sci. Technol.* **2016**, *6*, 41–48; (c) Bauer, I.; Knölker, H.-J. *Chem. Rev.* **2015**, *115*, 3170–3387; (d) Ollevier, T.; Keipour H. In: Bauer, E. *Iron Catalysis II*; Springer: Heidelberg, **2015**, pp. 259-310; (e)

Gopalaiah, K. *Chem. Rev.* **2013**, *113*, 3248–3296; (f) Darwish, M.; Wills, M. *Catal. Sci. Technol.* **2012**, *2*, 243–255; (g) Plietker, B. *Iron Catalysis I*; Springer: Heidelberg, **2011**; (h) Bolm, C. *Nature Chem.* **2009**, *1*, 420; (i) Fürstner, A. *Angew. Chem., Int. Ed.* **2009**, *48*, 1364–1367; (j) Enthaler, S.; Junge, K.; Beller, M. *Angew. Chem., Int. Ed.* **2008**, *47*, 3317–3321; (k) Correa, A.; Garcia Mancheno, O.; Bolm, C. *Chem. Soc. Rev.* **2008**, *37*, 1108–1117; (l) Bolm, C.; Legros, J.; Le Paih, J.; Zani, L. *Chem. Rev.* **2004**, *104*, 6217–6254.

5. Fusi, G. M.; Gazzola, S.; Piarulli, U. *Adv. Synth. Catal.*, **2022**, *364*, 696–714.

6. (a) Ho, T.-L. *Tandem Organic Reactions*; Wiley: New York; **1992**; (b) Bunce, R. A. *Tetrahedron* **1995**, *51*, 13103–13159; (c) Padwa, A.; Weingarten, M. D. *Chem. Rev.* **1996**, *96*, 223–270; (d) Denmark, S. E.; Thorarensen, A. *Chem. Rev.* **1996**, *96*, 137–165; (e) Hulme, C.; Gore, V. *Curr. Med. Chem.* **2003**, *10*, 51–80; (f) Tietze, L. F.; Rackelmann, N. *Pure Appl. Chem.* **2004**, *76*, 1967–1983; (g) Fogg, D. E.; dos Santos, E. N. *Coord. Chem. Rev.* **2004**, *248*, 2365–2379; (h) Wasilke, J.-C.; Obrey, S. J.; Baker, R. T.; Bazan, G. C. *Chem. Rev.* **2005**, *105*, 1001–1020; (i) Nicolaou, K. C.; Edmonds, D. J.; Bulger, P. G. *Angew. Chem., Int. Ed.* **2006**, *45*, 7134–7186; (j) Chapman, C. J.; Frost, C. G. *Synthesis* **2007**, *2007*, 1–21; (k) Padwa, A.; Bur, S. K. *Tetrahedron* **2007**, *63*, 5341–5378; (l) D'Souza, D. M.; Müller, T. J. J. *Chem. Soc. Rev.* **2007**, *36*, 1095–1108; (m) Alba, A.-N.; Companyo, X.; Viciano, M.; Rios, R. *Curr. Org. Chem.* **2009**, *13*, 1432–1474; (n) *Chem. Soc. Rev.* *38*, **2009**, Special Issue on Rapid formation of molecular complexity in organic synthesis; (o) Nicolaou, K. C.; Chen, J. S. *Chem. Soc. Rev.* **2009**, *38*, 2993–3009; (p) Ruiz, M.; Lopez-Alvarado, P.; Giorgi, G.; Menéndez, J. C. *Chem. Soc. Rev.* **2011**, *40*, 3445–3454; (q) De Graaff, C.; Ruijter, E.; Orru, R. V. A. *Chem. Soc. Rev.* **2012**, *41*, 3969–4009; (r) Pellissier, H. *Tetrahedron* **2013**, *69*, 7171–7210; (s) Pellissier, H. *Enantioselective Multicatalysed Tandem Reactions*; Royal Society of Chemistry: Cambridge, **2014**; (t) Ardkhean, R.; Caputo, D. F. J.; Morrow, S. M.; Shi, H.; Xiong, Y.; Anderson, E. A. *Chem. Soc. Rev.* **2016**, *45*, 1557–1569; (u) Pellissier, H. *Curr. Org. Chem.* **2016**, *20*, 234–265; (v) Hayashi, Y. *Chem. Sci.* **2016**, *7*, 866–880; (w) Pellissier, H. *Adv. Synth. Catal.* **2020**, *362*, 2289–2325.

7. (a) Posner, G. H. *Chem. Rev.* **1986**, *86*, 831–844; (b) Tietze, L. F.; Beifuss, U. *Angew. Chem., Int. Ed.* **1993**, *32*, 131–163; (c) Tietze, L. F. *Chem. Rev.* **1996**, *96*, 115–136; (d) Parsons, P. J.; Penkett, C. S.; Shell, A. J. *Chem. Rev.* **1996**, *96*, 195–206; (e) Dalko, P. I.; Moisan, L. *Angew. Chem., Int. Ed.* **2004**, *43*, 5138–5175; (f) Ramon, D. J.; Yus, M. *Angew.*

Chem., Int. Ed. **2005**, *44*, 1602–1634; (g) Zhu, J.; Bienaymé, H. *Multicomponent Reactions*, Wiley-VCH: Weinheim, **2005**; (h) Tietze, L. F.; Brasche, G.; Gericke, K. *Domino Reactions in Organic Synthesis*, Wiley-VCH: Weinheim, **2006**; (i) Pellissier, H. *Tetrahedron* **2006**, *62*, 2143–2173; (j) Pellissier, H. *Tetrahedron* **2006**, *62*, 1619–1665; (k) Enders, D.; Grondal, C.; Hüttl, M. R. M. *Angew. Chem., Int. Ed.* **2007**, *46*, 1570–1581; (l) Guillena, G.; Ramon, D. J.; Yus, M. *Tetrahedron: Asymmetry* **2007**, *18*, 693–700; (m) Touré, B. B.; Hall, D. G. *Chem. Rev.* **2009**, *109*, 4439–4486; (n) Orru, R. V. A.; Ruijter, E. *Synthesis of Heterocycles via Multicomponent Reactions, Topics in Heterocyclic Chemistry*, Vols. I and II, Springer: Berlin, **2010**; (o) Pellissier, H. *Adv. Synth. Catal.* **2012**, *354*, 237–294; (p) Clavier, H.; Pellissier, H. *Adv. Synth. Catal.* **2012**, *354*, 3347–3403; (q) Pellissier, H. *Chem. Rev.* **2013**, *113*, 442–524; (r) Pellissier, H. *Asymmetric Domino Reactions*, Royal Society of Chemistry: Cambridge, **2013**; (s) Tietze, L. F. *Domino Reactions - Concepts for Efficient Organic Synthesis*, Wiley-VCH: Weinheim, **2014**; (t) J. Zhu, Q. Wang, M. Wang, *Multicomponent Reactions in Organic Synthesis*, Wiley: Weinheim, **2014**; (u) Herrera, R. P.; Marques-Lopez, E. *Multicomponent Reactions: Concepts and Applications for Design and Synthesis*, Wiley: Weinheim, **2015**; (v) Snyder, S. A. *Science of Synthesis. Applications of Domino Transformations in Organic Synthesis*, Thieme Verlag: Stuttgart, **2016**, Vols 1-2; (w) Pellissier, H. *Adv. Synth. Catal.* **2016**, *358*, 2194–2259; (x) Pellissier, H. *Curr. Org. Chem.* **2018**, *22*, 2670–2697; (y) Pellissier, H. *Synthesis*, **2019**, *51*, 1311–1318; (z) Pellissier, H. *Org. Prep. Proc. Int.* **2019**, *51*, 311–344; (aa) Pellissier, H. *Adv. Synth. Catal.* **2019**, *361*, 1733–1755; (ab) Pellissier, H. *Asymmetric Metal Catalysis in Enantioselective Domino Reactions*, Wiley: Weinheim, **2019**; (ac) Pellissier, H. *Synthesis* **2020**, *52*, 3837–3854; (ad) Pellissier, H. *Curr. Org. Chem.* **2021**, *25*, 1457–1471; (ae) Pellissier, H. *Adv. Synth. Catal.* **2023**, *365*, 620–681; (af) Pellissier, H. *Adv. Synth. Catal.* **2023**, *365*, 768–819.

8. Li, W.; Zhou, P.; Li, G.; Lin, L.; Feng, X. *Adv. Synth. Catal.* **2020**, *362*, 1982–1987.

9. Oguma, T.; Doiuchi, D.; Fujitomo, C.; Kim, C.; Hayashi, H.; Uchida, T.; Katsuki, T. *Asian J. Org. Chem.* **2020**, *9*, 404–415.

10. (a) Chen, C.; Wang, H.; Sun, Y.; Cui, J.; Xie, J.; Shi, Y.; Yu, S.; Hong, X.; Lu, Z. *iScience* **2020**, *23*, 100985; (b) Guo, J.; Cheng, Z.; Chen, J.; Chen, X.; Lu, Z. *Acc. Chem. Res.* **2021**, *54*, 2701–2716.

-
11. Liu, L.; Lee, W.; Yuan, M.; Acha, C.; Geherty, M. B.; Williams, B.; Gutierrez, O. *Chem. Sci.* **2020**, *11*, 3146–3151.
 12. Liu, W.; Pu, M.; He, J.; Zhang, T.; Dong, S.; Liu, X.; Wu, Y.-D.; Feng, X. *J. Am. Chem. Soc.* **2021**, *143*, 11856–11863.
 13. Ge, L.; Zhou, H.; Chiou, M.-F.; Jiang, H.; Jian, W.; Ye, C.; Li, X.; Zhu, X.; Xiong, H.; Li, Y.; Song, L.; Zhang, X.; Bao, H. *Nature Catal.* **2021**, *4*, 28–35.
 14. Lv, D.; Sun, Q.; Zhou, H.; Ge, L.; Qu, Y.; Li, T.; Ma, X.; Li, Y.; Bao, H. *Angew. Chem., Int. Ed.* **2021**, *60*, 12455–12460.
 15. Youshaw, C. R.; Yang, M.-H.; Gogoi, A. R.; Rentería-Gómez, A.; Liu, L.; Morehead, L. M.; Gutierrez, O. *Org. Lett.* **2023**, *25*, 8320–8325.
 16. De Luca, L.; Mezzetti, A. *J. Org. Chem.* **2020**, *85*, 5807–5814.
 17. Huo, S.; Wang, Q.; Zuo, W. *Dalton Trans.* **2020**, *49*, 7959–7967.
 18. Xue, Q.; Wu, R.; Wang, D.; Zhu, M.; Zuo, W. *Organometallics* **2021**, *40*, 134–147.
 19. (a) Lu, P.; Lu, Z. *Synthesis* **2023**, *55*, 1042–1052; (b) Behera, P.; Ramakrishna, D. S.; Chandrasekhar, M. M.; Kothakapu, S. R. *Chirality* **2023**, *35*, 477–497.
 20. Yang, L.; Tan, X.; Zhao, M.; Wen, J.; Zhang, X. *Chem. Eur. J.* **2023**, *29*, e202301609.
 21. Newar, R.; Akhtar, N.; Antil, N.; Kumar, A.; Shukla, S.; Begum, W.; Manna, K. *Angew. Chem., Int. Ed.* **2021**, *60*, 10964–10970.
 22. Antil, N.; Akhtar, N.; Newar, R.; Begum, W.; Kumar, A.; Chauhan, M.; Manna, K. *ACS Catal.* **2021**, *11*, 10450–10459.
 23. Blasius, C. K.; Heinrich, N. F.; Vasilenko, V.; Gade, L. H. *Angew. Chem., Int. Ed.* **2020**, *59*, 15974–15977.
 24. Sathish, M.; Nachtigall, F. M.; Santos, L. S. *Org. Lett.* **2022**, *24*, 7627–7634.
 25. Braconi, E.; Götzinger, A. C.; Cramer, N. *J. Am. Chem. Soc.* **2020**, *142*, 19819–19824.
 26. Ping, Y.-J.; Zhou, Y.-M.; Wu, L.-L.; Li, Z.-R.; Gu, X.; Wan, X.-L.; Xu, Z.-J.; Che, C.-M. *Org. Chem. Front.* **2021**, *8*, 1910–1917.

-
27. Hong, Y.; Cui, T.; Ivlev, S.; Xie, X.; Meggers, E. *Chem. Eur. J.* **2021**, *27*, 8557–8563.
28. Braconi, E.; Cramer, N. *Angew. Chem., Int. Ed.* **2022**, *61*, e202112148.
29. Chen, K.-G.; Lu, H.; Zhou, Y.-M.; Wan, X.-L.; Wang, H.-Y.; Xu, Z.-J.; Guo, H. M.; Che, C.-M. *J. Org. Chem.* **2022**, *87*, 8289–8302.
30. Lauzon, S.; Schouwey, L.; Ollevier, T. *Org. Lett.* **2022**, *24*, 1116–1120.
31. Lu, H.; Chen, K.-G.; Li, G.-X.; Zhan, K.; Xu, Z.-J.; Che, C.-M. *Org. Chem. Front.* **2023**, *10*, 2054–2060.
32. Wei, J.; Wu, L.; Wang, H.-X.; Zhang, X.; Tse, C.-W.; Zhou, C.-Y.; Huang, J.-S.; Che, C.-M. *Angew. Chem., Int. Ed.* **2020**, *59*, 16561–16571.
33. Chen, J.; Luo, X.; Sun, Y.; Si, S.; Xu, Y.; Lee, Y.-M.; Nam, W.; Wang, B. *CCS Chem.* **2022**, *4*, 2369–2381.
34. (a) Yudin, A. *Aziridines and Epoxides in Organic Synthesis*; Wiley-VCH: Weinheim, **2006**, Chaps. 7-9; (b) Johnson, J. B. In: De Vries, J. G.; Molander, G. A.; Evans, P. A. *Science of Synthesis, Stereoselective Synthesis*; Vol. 3, Georg Thieme: Stuttgart, **2011**, pp 759-827; (c) Pellissier, H.; Lattanzi, A., Dalpozzo, R. *Asymmetric Synthesis of Three-Membered Rings*; Wiley: Weinheim, **2017**; (d) Dalpozzo, R.; Lattanzi, A.; Pellissier, H. *Curr. Org. Chem.* **2017**, *21*, 1143–1191.
35. Li, Y.; Zhang, Y.; Zhang, H.-Y.; Han, Y.-P.; Zhao, J. *Asian J. Org. Chem.* **2020**, *9*, 616–622.
36. Viereck, P.; Rummelt, S. M.; Soja, N. A.; Pabst, T. P.; Chirik, P. J. *Organometallics* **2021**, *40*, 1053–1061.
37. Lu, P.; Ren, X.; Xu, H.; Lu, D.; Sun, Y.; Lu, Z. *J. Am. Chem. Soc.* **2021**, *143*, 12433–12438.
38. Adak, L.; Jin, M.; Saito, S.; Kawabata, T.; Itoh, T.; Ito, S.; Sharma, A. K.; Gower, N. J.; Cogswell, P.; Geldsetzer, J.; Takaya, H.; Isozaki, K.; Nakamura, M. *Chem. Commun.* **2021**, *57*, 6975–6978.
39. Shu, T.; Cossy, J. *Chem. Eur. J.* **2021**, *27*, 11021–11029.

-
40. Wu, L.-Y.; Usman, M.; Liu, W.-B. *Molecules* **2020**, *25*, 852–861.
41. (a) Tyrol, C. C.; Yone, N. S.; Gallin, C. F.; Byers, J. A. *Chem. Commun.* **2020**, *56*, 14661–14664; (b) Tyrol, C. C.; Yone, N.; Gallina, C. F.; Byers, J. A. *ChemRxiv* **2020**, 1–6.
42. Dyadyuk, A.; Vershinin, V.; Shalit, H.; Shalev, H.; More, N. Y.; Pappo, D. *J. Am. Chem. Soc.* **2022**, *44*, 3676–3684.
43. Surgenor, R. R.; Liu, X.; Keenlyside, M. J. H.; Myers, W.; Smith, M. D. *Nature Chem.* **2023**, *15*, 357–365.
44. Ying, P.; Ying, T.; Chen, H.; Xiang, K.; Yu, J. *Org. Chem. Front.* **2024**, *11*, 127–134.
45. Wei, J.; Huang, J.-S.; Che, C.-M. *Org. Lett.* **2021**, *23*, 6993–6997.
46. He, C.; Wu, Z.; Zhou, Y.; Cao, W.; Feng, X. *Org. Chem. Front.* **2022**, *9*, 703–708.
47. Ye, C.-X.; Shen, X.; Chen, S.; Meggers, E. *Nature Chem.* **2022**, *14*, 566–573.
48. Ye, C.-X.; Dansby, D. R.; Chen, S.; Meggers, E. *Nat. Synth.* **2023**, *2*, 645–652.
49. Xu, N.; Pu, M.; Yu, H.; Yang, G.; Liu, X.; Feng, X. *Angew. Chem., Int. Ed.* **2024**, *63*, e202314256.
50. (a) Pellissier, H. *Tetrahedron* **2007**, *63*, 1297–1330; (b) Mellah, M.; Voituriez, A.; Schulz, E. *Chem. Rev.* **2007**, *107*, 5133–5209; (c) Sipos, G.; Drinkel, E. E.; Dorta, R. *Chem. Soc. Rev.* **2015**, *44*, 3834–3860; (d) Otocka, S.; Kwiatkowska, M.; Madalinska, L.; Kielbasinski, P. *Chem. Rev.* **2017**, *117*, 4147–4181.
51. (a) Carreno, M. C. *Chem. Rev.* **1995**, *95*, 1717–1760; (b) Pellissier, H. *Tetrahedron* **2006**, *62*, 5559–5601; (c) Carreno, M. C.; Hernandez-Torres, G.; Ribagorda, M.; Urbano, A. *Chem. Commun.* **2009**, 6129–6144; (d) Kaiser, D.; Klose, I.; Oost, R.; Neuhaus, J.; Maulide, N. *Chem. Rev.* **2019**, *119*, 8701–8780.
52. (a) Bentley, R. *Chem. Soc. Rev.* **2005**, *34*, 609–624; (b) Legros, J.; Dehli, J. R.; Bolm, C. *Adv. Synth. Catal.* **2005**, *347*, 19–31.
53. (a) Fernandez, I.; Khair, N. *Chem. Rev.* **2003**, *103*, 3651–3706; (b) Wojaczynska, E.; Wojaczynski, J. *Chem. Rev.* **2010**, *110*, 4303–4356; (c) O’Mahony, G. E.; Ford, A.; Maguire, A. R. *J. Sulfur Chem.* **2013**, *34*, 301–341; (d) Han, J.; Soloshonok, V. A.; Klika, K. D.; Drabowicz, J.; Wzorek, A. *Chem. Soc. Rev.*, **2018**, *47*, 1307–1350.

-
54. Wang, F.; Feng, L.; Dong, S.; Liu, X.; Feng, X. *Chem. Commun.* **2020**, *56*, 3233–3236.
55. Gilissen, P. J.; Chen, X.; De Graaf, J.; Tinnemans, P.; Feringa, B. L.; Elemans, J. J. A. W.; Nolte, R. J. M. *Chem. Eur. J.* **2023**, *29*, e202203539.
56. Wei, J.; Cao, B.; Tse, C.-W.; Chang, X.-Y.; Zhou, C.-Y.; Che, C.-M. *Chem. Sci.* **2020**, *11*, 684–693.
57. Wang, L.; Zhou, P.; Lin, Q.; Dong, S.; Liu, X.; Feng, X. *Chem. Sci.* **2020**, *11*, 10101–10106.
58. Steinlandt, P. S.; Xie, X.; Ivlev, S.; Meggers, E. *ACS Catal.* **2021**, *11*, 7467–7476.
59. Steinlandt, P. S.; Hemming, M.; Xie, X.; Ivlev, S. I.; Meggers, E. *Chem. Eur. J.* **2023**, *29*, e202300267.
60. Wang, H.-H.; Shao, H.; Huang, G.; Fan, J.; To, W.-P.; Dang, L.; Liu, Y.; Che, C.-M. *Angew. Chem., Int. Ed.* **2023**, *62*, e202218577.
61. Cui, T.; Ye, C.-X.; Thelemann, J.; Jenisch, D.; Meggers, E. *Chin. J. Chem.* **2023**, *41*, 2065–2070.
62. Zhou, Y.-M.; Ping, Y.-J.; Xu, Z.-J.; Che, C.-M. *Asian J. Org. Chem.* **2021**, *10*, 674–678.
63. Wang, K.; Li, Y.; Li, X.; Li, D.; Bao, H. *Org. Lett.* **2021**, *23*, 8847–8851.
64. Lai, C.; Lebel, H. *Helv. Chim. Acta* **2022**, *105*, e202100209.
65. Guan, H.; Tung, C.-H.; Liu, L. *J. Am. Chem. Soc.* **2022**, *144*, 5976–5984.